NACA TN 2733 9606

TECH LIBRARY KAFB, NM
0065781

NATIONAL ADVISORY COMMITTEE FOR AERONAUTICS

TECHNICAL NOTE 2733

METHOD FOR CALCULATION OF HEAT TRANSFER IN LAMINAR REGION OF AIR FLOW AROUND CYLINDERS OF ARBITRARY CROSS SECTION (INCLUDING LARGE TEMPERATURE DIFFERENCES AND TRANSPIRATION COOLING)

By E. R. G. Eckert and John N. B. Livingood

Lewis Flight Propulsion Laboratory
Cleveland, Ohio

Washington
June 1952

AFMDC
TECHNICAL LIBRARY
AFL 2811

TECH LIBRARY KAFB, NM
0065781

1S

2447

NATIONAL ADVISORY COMMITTEE FOR AERONAUTICS

TECHNICAL NOTE 2733

METHOD FOR CALCULATION OF HEAT TRANSFER IN LAMINAR REGION OF AIR FLOW AROUND CYLINDERS OF ARBITRARY CROSS SECTION (INCLUDING LARGE TEMPERATURE DIFFERENCES AND TRANSPIRATION COOLING)

By E. R. G. Eckert and John N. B. Livingood

SUMMARY

The solution of heat-transfer problems has become vital for many aeronautical applications. The shapes of objects to be cooled can often be approximated by cylinders of various cross sections with flow normal to the axis as, for instance, heat transfer on gas-turbine blades and on airfoils heated for deicing purposes. A laminar region always exists near the stagnation point of such objects.

A method previously presented by E. R. G. Eckert permits the calculation of local heat transfer around the periphery of cylinders of arbitrary cross section in the laminar region for flow of a fluid with constant property values with an accuracy sufficient for engineering purposes. The method is based on exact solutions of the boundary-layer equations for incompressible wedge-type flow and on the postulate that on any location of the cylinder the boundary-layer growth is the same as that on a wedge with comparable flow conditions. This method is extended herein to take into account the influence of large temperature differences between the cylinder wall and the flow as well as the influence of transpiration cooling when the same medium as in the outside flow is used as coolant. Prepared charts make the calculation procedure very rapid. For cylinders with solid walls and elliptic cross section, a comparison is made between the results of calculations based on the presented method and the results of calculations by other known methods as well as of experimental investigations.

INTRODUCTION

A calculation of heat transfer to cylinders with arbitrary cross section in an air flow normal to the axis by a solution of the boundary-layer equations is a difficult problem, even for the laminar region. The problem is especially complicated by the large number of parameters

influencing heat transfer. Such parameters are the shape of the cross section of the cylinder, the Mach number which determines the flow outside the boundary layer, the temperatures on the surface of the cylinder as well as in the stream, the stream velocity determining the internal heat generation, and the temperature distribution around the circumference of the cylinder. If the cylinder is cooled by the transpiration-cooling method in which a coolant is ejected through the porous surface into the outside stream, the amount of coolant and its distribution around the circumference of the cross section of the cylinder are additional parameters. Even if a solution is obtained for such a problem, for instance by use of an electronic computer, this solution is very restricted because of the many parameters. Up to the present time, therefore, the problem has been attacked only under simplifying restrictions.

2447

The restrictions most commonly used are: (1) low velocities, (2) constant property values, (3) constant wall temperatures, and (4) impermeable surfaces (no transpiration cooling). Under restriction (2), the development of the boundary layer along the cylindrical surface is independent of the heat transfer; available knowledge on the flow boundary layer can therefore be used as a basis for a heat-transfer calculation. Under the simplifying assumptions, which are necessary in order to transform the general viscous-flow equations into the boundary-layer equations, the development of the flow boundary layer does not depend immediately on the shape of the cross section of the cylinder, but only on the velocity distribution in the stream outside the boundary layer and along its surface.

One method which was applied successfully to obtain a solution of the flow boundary-layer equation developed the stream velocity along the surface of the cylinder in a power series of the distance from the stagnation point measured along the circumference of the cylinder. In reference 1 this method is used to solve the heat-transfer problem. It is also shown that the temperature field within the boundary layer can also be presented in a power series of the distance from the stagnation point in which the single terms contain only universal functions of a dimensionless wall distance and of the Prandtl number of the fluid. The heat transfer to the surface is given by an analogous series with terms depending on the Prandtl number. The calculation of the universal functions, however, is a tedious process, and accordingly these functions are known only for a limited number of terms. For air with a Prandtl number of 0.7, they are presented in reference 1. For a gas with a Prandtl number of 1, they are contained in reference 2, which is based on reference 3, in which the boundary-layer flow of a yawed cylinder is calculated. The fact that the boundary-layer equation for the velocity component parallel to the axis of a yawed cylinder is identical in form to the boundary-layer equation describing the temperature field for a fluid with a Prandtl number of 1, flowing normal to the axis of the

cylinder, was used in reference 2 to determine heat transfer to such cylinders. The presentation of more terms of the series is announced in reference 4. It is found, however, that the velocity distribution for only a limited range of cross sections of cylinders can be represented by a power series converging rapidly enough that the number of the known universal functions is sufficient to calculate the heat transfer.

The difficulties connected with a solution of the boundary-layer equations point out the need for an approximate approach which, with a small expenditure of time, would determine heat-transfer coefficients with an accuracy sufficient for engineering purposes. A considerable number of such approaches were tried in the past with results which differ greatly as shown in figure 1, taken from reference 2.

2447

The simplest procedure is probably the use of the heat-transfer coefficients as calculated in reference 5 for flow along a flat plate with a constant velocity. The fact that in reality the stream velocity varies along the cross section of the cylinder is taken into account by calculating the local heat-transfer coefficients with the velocity found in the stream at the considered distance from the stagnation point. This method is contained in a summary presented in reference 6. Unfortunately, such an approach gives heat-transfer coefficients which are considerably low in many cases (see fig. 1).

Better agreement was obtained by another approach (reference 7) which uses, instead of the flat-plate solution, a family of solutions of the boundary-layer equations which can be obtained in a general form, namely, for the case where the stream velocity varies along the surface as a certain power of the distance from the stagnation point. Such a velocity variation is obtained in incompressible flow around wedges. The solutions for such a type of flow were used to obtain approximate heat-transfer coefficients for a cylinder with arbitrary cross section by stipulating that the local heat-transfer coefficient on any location along the cylinder is identical to the local heat-transfer coefficient on a wedge for which, at the same distance from the stagnation point, the stream velocity and its gradient are the same as those on the investigated cylinder. This approach was subsequently used by different authors, and is described, for instance, in references 8 and 9. It takes into account the stream conditions which influence the boundary-layer growth at the location at which the heat transfer is going to be determined; however, it does not properly account for the development of the boundary layer in the range upstream of the point considered. This development may be different on the cylinder and on the equivalent wedge.

Another group uses an integrated momentum equation for the boundary-layer flow as proposed by von Kármán and K. Pohlhausen (references 10 and 11) to calculate the velocity boundary layer. Different procedures were proposed to determine local heat-transfer coefficients from the

known velocity boundary layer. Some investigators use Reynolds analogy directly (reference 12) or with a correction for Prandtl numbers different from 1 (reference 13). Such approaches give heat-transfer coefficients which are considerably high in many cases, as shown, for instance, in figure 1. More accurate results were obtained when the heat transfer was determined by solving an integrated heat-flow equation for the boundary layer. The velocity field within the boundary layer has to be known in this approach, since the flow velocities within the boundary layer occur in the mentioned heat-flow equation. This method was originated by Kroujiline (reference 14). Extensions and simplifications are contained in references 15 to 18 and an extension to compressible flow of a fluid with a Prandtl number equal to 1 is found in references 19 and 20. Useful information is also contained in a summarizing report (reference 21). 2447

Another approach starts from a consideration of the fact that the use of the heat-transfer coefficients for wedge-type profiles as described previously was found to give heat-transfer coefficients with a fairly good accuracy. It should be expected that these heat-transfer coefficients can be improved to a degree which is sufficient for all engineering purposes by a method which takes into account in some approximate way the previous history of the boundary layer. Such a method, called the equivalent wedge-type flow method, was proposed in reference 22, extended to heat transfer at high flow velocities and variable wall temperature in reference 23, and extended to transpiration cooling with small temperature differences in reference 24. The advantages of this method are that no knowledge of the velocity boundary layer is required and that it can be readily extended to take into account the effects of large temperature differences, of transpiration cooling, and of variable wall temperature as soon as the corresponding solutions for the wedge-type flow are available.

This report presents such an extension, made at the NACA Lewis laboratory, which includes the effects of large temperature differences and of transpiration cooling. It is based on exact boundary-layer solutions for wedge-type flow with large temperature differences and with transpiration cooling (reference 25). Charts were prepared which make the calculation of heat transfer around cylinders of any arbitrary cross section more rapid.

SOLUTION OF BOUNDARY-LAYER EQUATIONS FOR WEDGE-TYPE FLOW

Boundary-Layer Equations

The following boundary-layer equations describe the velocity and temperature fields in a laminar steady two-dimensional gas flow: the momentum equation, the continuity equation, and the energy equation. The momentum equation is

$$\rho u \frac{\partial u}{\partial x} + \rho v \frac{\partial u}{\partial y} = \frac{\partial}{\partial y}\left(\mu \frac{\partial u}{\partial y}\right) - \frac{\partial p}{\partial x} \tag{1}$$

when body forces are neglected. (All symbols are defined in appendix A; consistent units are used throughout the report.) Since the pressure variation normal to the surface throughout the boundary layer may be neglected, it follows that the pressure is prescribed by the conditions in the stream outside the boundary layer and can be connected with the velocity u_s in the stream and just outside the boundary layer by the Bernoulli equation

2447

$$-\frac{\partial p}{\partial x} = \rho_s u_s \frac{\partial u_s}{\partial x}$$

The introduction of this expression changes the momentum equation to the form

$$\rho u \frac{\partial u}{\partial x} + \rho v \frac{\partial u}{\partial y} = \frac{\partial}{\partial y}\left(\mu \frac{\partial u}{\partial y}\right) + \rho_s u_s \frac{\partial u_s}{\partial x} \tag{2}$$

The continuity equation is

$$\frac{\partial}{\partial x}(\rho u) + \frac{\partial}{\partial y}(\rho v) = 0 \tag{3}$$

and the energy equation is

$$\rho c_p \left(u \frac{\partial T}{\partial x} + v \frac{\partial T}{\partial y}\right) = \frac{\partial}{\partial y}\left(k \frac{\partial T}{\partial y}\right) + \mu \left(\frac{\partial u}{\partial y}\right)^2 + u \frac{\partial p}{\partial x} \tag{4}$$

The heat generated by internal friction, described by the second term on the right side of equation (4), and the temperature variation connected with expansion, described by the third term, can be neglected as long as the difference between the total and the static temperature in the gas stream is small compared with the difference between the wall temperature and the temperature in the gas stream. For this condition, then, only the first term on the right side of equation (4) is retained, and the energy equation assumes the form

$$\rho c_p \left(u \frac{\partial T}{\partial x} + v \frac{\partial T}{\partial y}\right) = \frac{\partial}{\partial y}\left(k \frac{\partial T}{\partial y}\right) \tag{5}$$

Equations (2), (3), and (5) include the case of transpiration cooling when the same medium as that in the outside flow is used as coolant and the boundary conditions are properly defined.

$$u = 0, \; v = v_w, \quad \text{and} \quad T = T_w \quad \text{when} \quad y = 0$$
$$u \rightarrow u_s \quad \text{and} \quad T \rightarrow T_s \quad \text{when} \quad y \rightarrow \infty \tag{6}$$

The property values μ, k, c_p, and ρ appearing in the equations depend on temperature and pressure. The variation with pressure can be neglected at the small velocities to which the energy equation was already restricted by disregarding the internal friction and the expansion terms. The influence of the temperature dependency, however, may be appreciable in applications with large temperature differences within the boundary layer. Solutions of the boundary-layer equations which take into account the temperature variation of the property values were obtained in references 9 and 25, in which the partial differential equations were transformed into total differential equations. 2447

Change of Variables

The transformation of the partial differential equations into total differential equations is possible under the following specialized conditions: The stream velocity is assumed to vary as a power function of the distance from the stagnation point measured along the surface of the cylinder.

$$u_s = Cx^m \tag{7}$$

It has recently become customary to refer to the exponent m in this equation as "Euler number." The Euler number can be expressed by the Bernoulli equation in the following way:

$$m = \frac{-\frac{\partial p}{\partial x}}{\frac{\rho_s u_s^2}{x}} \tag{8}$$

In addition, the temperature of the wall is assumed to be constant and the property values are assumed to vary proportionally to a power of the absolute temperature T. The numerical calculations were made for air. The exponents used were 0.7 for the viscosity, 0.85 for the heat conductivity, 0.19 for the specific heat, and -1.0 for the density. The variables

2447

$$\left.\begin{aligned} \eta &= y\sqrt{\frac{\rho_w u_s}{\mu_w x}} \\ f &= \frac{\rho_w \psi}{\sqrt{\mu_w \rho_w x u_s}} \\ \theta &= \frac{T - T_w}{T_s - T_w} \end{aligned}\right\} \tag{9}$$

are used to transform equations (2), (3), and (5) into total differential equations presenting f and θ as functions of η only. The stream function ψ appearing in equations (9) is defined in such a way as to eliminate the continuity equation (3).

$$\left.\begin{aligned} \rho u &= \frac{\partial(\rho_w \psi)}{\partial y} \\ \rho v &= -\frac{\partial(\rho_w \psi)}{\partial x} \end{aligned}\right\} \tag{10}$$

Introducing the new variables into the second of equations (10) leads to the following expression for the velocity component normal to the surface:

$$-\rho v = \rho_w \left[\frac{1+m}{2} f \sqrt{\frac{\mu_w u_s}{\rho_w x}} + \frac{y}{2} f' (m-1) \frac{u_s}{x}\right] \tag{11}$$

The velocity at the surface itself follows:

$$v_w = -\frac{1+m}{2} f_w \sqrt{\frac{\mu_w u_s}{\rho_w x}} \tag{12}$$

The transformation therefore prescribes a certain variation of the coolant velocity v_w along the surface, since the function f_w has to be constant (independent of x). Since the stream velocity is described by equation (7), the coolant velocity v_w is also proportional to some power of x. It is shown in reference 26 that such a variation of the coolant velocity leads to a constant wall temperature and is therefore consistent with the assumed constant wall temperature when heat transfer by radiation may be neglected. The transformed equations are presented in references 9 and 25, together with the solutions for a Prandtl number Pr of 0.7, and for a range of Euler number m, temperature ratio T_s/T_w, and the parameter f_w describing the cooling-air flow through

the porous surface. The results contain expressions for the thickness of the flow boundary layer which are defined in two ways: the displacement thickness

$$\delta_d = \int_0^\infty \left(1 - \frac{\rho u}{\rho_s u_s}\right) dy \tag{13}$$

and the momentum thickness

$$\delta_i = \int_0^\infty \frac{\rho u}{\rho_s u_s} \left(1 - \frac{u}{u_s}\right) dy \tag{14}$$

2447

The thermal boundary layer is characterized in this report by the convection thickness

$$\delta_c = \int_0^\infty \frac{\rho u}{\rho_s u_s} \frac{T - T_s}{T_w - T_s} dy \tag{15}$$

In addition, a thermal boundary-layer thickness will be used herein and is defined in the following way:

$$\delta_t = \int_0^\infty \left(\frac{T - T_s}{T_w - T_s}\right) dy \tag{16}$$

Values for this boundary-layer thickness can be easily calculated from results presented in reference 25.

Application to High Velocities

The solutions described apply exactly only to flow with small velocities. Practically, the limiting velocity up to which it is possible to neglect the frictional and the expansion terms can be set quite high for a gas; this fact can be understood from the following transformation of the energy equation, in which only the specific heat is regarded constant. If the momentum equation (1) is multiplied by the velocity u and added to the energy equation (4) and if, in addition, the total temperature $T_T = T + u^2/2c_p$ is introduced, the following expression is obtained:

$$\rho c_p \left(u \frac{\partial T_T}{\partial x} + v \frac{\partial T_T}{\partial y}\right) = \frac{\partial}{\partial y}\left(k \frac{\partial T_T}{\partial y}\right) + \frac{1}{2}\frac{\partial}{\partial y}\left[\mu\left(1 - \frac{1}{Pr}\right)\frac{\partial(u^2)}{\partial y}\right] \tag{17}$$

The last term on the right side of the equation vanishes for a Prandtl number equal to 1. In this case, the energy equation has the same form as the one for low velocities in which the friction and the expansion terms were neglected. The only difference lies in the fact that the total temperature appears in the energy equation. For cases which have a Prandtl number not too far from 1, the last term in equation (17) will be comparatively small up to considerable velocities, and the energy equation (5) used in the following considerations applies to this condition when the temperature T is interpreted as total temperature. It will be shown later that as far as heat transfer is concerned, the range in which the results of a calculation with equation (5) may be used can be extended even further by using a properly defined adiabatic wall temperature instead of the total gas temperature.

2447

The property values μ, k, c_p, and ρ depend for gases on the temperature. This dependency was taken into account in the described calculations. The density depends, in addition, on the pressure, and the pressure variation may become considerable at high Mach numbers. There are indications, however, that calculations which neglect this pressure variation can be used with sufficient accuracy over the whole subsonic range, as is pointed out in reference 27 by an investigation of results obtained by L. Howarth (reference 28).

EXTENSION OF THEORY TO ARBITRARY BODIES

Determination of Equivalent Wedge

The solutions discussed in the previous paragraph are in an exact sense restricted to a certain type of velocity variation along the cylindrical surface, namely, a stream velocity which just outside the boundary layer is proportional to some power of the distance from the stagnation point. Such a velocity distribution is realized, for instance, in incompressible flow around wedges. The wedge-type solutions may be used, however, to obtain approximate heat-transfer coefficients on cylinders of arbitrary cross section. One approach in this direction assumes that the heat-transfer coefficient on any point along the circumference of a profile with arbitrary cross section is the same as that on a wedge at the same distance from the leading edge, provided the stream velocity and its gradient on the wedge and on the arbitrary profile have the same value at the location considered and that the temperature ratio T_s/T_w is the same. It will be shown that such an approach takes into account the right stream conditions at the local spot for which the heat-transfer coefficient is to be determined. However, it does not properly consider the previous history within the boundary layer. Numerical calculations presented later show that heat-transfer coefficients obtained in such a way are in most cases within

about 15-percent agreement with experimental data. It is to be expected that a modification which accounts in some approximate manner for the conditions in the boundary layer upstream of the point under consideration should improve this approximation to the desired degree. This modification is made in reference 22 by the stipulation that the rate of increase of the boundary-layer thickness is the same on the considered point of an arbitrary profile and on the point of a wedge which has the same boundary-layer thickness, the same stream velocity, and the same stream velocity gradient. This same stipulation will be used in the present report. For a given temperature ratio T_s/T_w, the heat-transfer coefficients on a wedge depend on the Euler number m and the value f_w characterizing the coolant flow through the porous surface. These parameters which define the equivalent wedge profile will now be expressed by the boundary-layer thickness and the local stream velocity gradient. 2447

For the wedge-type profile, the stream velocity is expressed by the power law

$$u_s = C\xi^m \tag{18}$$

in which the value ξ expresses the distance from the leading edge measured along the wedge surface in order to distinguish it from the distance of the point under consideration from the stagnation point on the arbitrary profile, which will be denoted by x. The variables used for the transformation of the original boundary-layer equations in the previous section may now be written

$$\eta = y\sqrt{\frac{\rho_w u_s}{\mu_w \xi}} \tag{19}$$

and

$$f_w = -\frac{2}{m+1} v_w \sqrt{\frac{\rho_w \xi}{\mu_w u_s}} \tag{20}$$

To a certain value y indicating the boundary-layer thickness δ belongs a value η_b of the coordinate η defined by the equation

$$\eta_b = \delta\sqrt{\frac{\rho_w u_s}{\mu_w \xi}} \tag{21}$$

In order to eliminate the distance ξ from this equation, equation (18) is differentiated to obtain

$$\frac{\partial u_s}{\partial \xi} = mC\xi^{m-1} = m\frac{u_s}{\xi} \tag{22}$$

Since the velocity gradient on the wedge profile is assumed the same as that on the profile under consideration, it follows that $\partial u_s/\partial \xi = \partial u_s/\partial x$. This equality gives for the coordinate ξ the expression

$$\xi = \frac{mu_s}{du_s/dx} \tag{23}$$

When this expression is introduced into equation (21), there is obtained

$$\eta_b = \delta\sqrt{\frac{\rho_w}{\mu_w m}\left(\frac{du_s}{dx}\right)}$$

In this expression, η_b (denoted as $(\delta/x)\sqrt{Re}$ in reference 25) is a function of the Euler number m and of the coolant-flow parameter f_w. If this equation is therefore written in the form

$$\eta_b^2 m = \frac{\rho_w \delta^2}{\mu_w}\frac{du_s}{dx} \tag{24}$$

the left side is a function of m and f_w and equation (24) relates both values to the boundary-layer thickness δ and the velocity gradient du_s/dx. In order to obtain a second relation for m and f_w, the coordinate ξ is replaced in equation (20). The result is

$$-\frac{m+1}{2} f_w \eta_b = \frac{\rho_w v_w \delta}{\mu_w} \tag{25}$$

which is written again in such a way that the left side is a function of the Euler number m and the flow parameter f_w, which can be calculated from the results in reference 25. Both equations (24) and (25) are therefore sufficient to determine the equivalent wedge profile.

Equations for Boundary-Layer Thickness and Heat Transfer

The next step is to develop a differential equation for the boundary-layer thickness from the postulate that the boundary-layer gradient $d\delta/dx$ is the same for the real profile as for the equivalent wedge profile. For the wedge profile, the boundary-layer thickness is given by the expression

$$\delta = \eta_b \sqrt{\frac{\mu_w}{C\rho_w}}\, \xi^{\frac{1-m}{2}}$$

2447

which is obtained from equation (21) by replacing the stream velocity with equation (18) and solving for the boundary-layer thickness. A differentiation of this equation and the use of equations (23) and (24) result in

$$\frac{d\delta}{dx} = \frac{1-m}{2m}\,\delta\,\frac{du_s/dx}{u_s} = \frac{1-m}{2}\,\eta_b{}^2\,\frac{\mu_w}{\rho_w \delta u_s} \tag{26}$$

This is a differential equation for the boundary-layer thickness which contains only values which are known for the profile under consideration or which are determined from equations (24) and (25) for the equivalent wedge-type flow. An integration of the differential equation gives the boundary layer along the circumference of the profile under consideration.

The local heat-transfer coefficient is defined by the following equation:

$$h(T_s - T_w) = k_w \left(\frac{\partial T}{\partial y}\right)_w$$

Introducing the dimensionless temperature ratio given in equation (9) and the coordinate ξ results in

$$h = k_w \theta_w' \frac{\partial \eta}{\partial y} = k_w \theta_w' \frac{\eta_b}{\delta} \tag{27}$$

The heat-transfer coefficient may be calculated from this expression as soon as the boundary-layer thickness δ is known, since θ_w' and η_b are functions of m and f_w contained in reference 25.

Up to the present time, no recommendation has been made as to which boundary-layer thickness should be used in the prescribed procedure. When the momentum thickness is used in the foregoing equations, it is easily understandable that the integrated momentum equation is satisfied and the method of calculation becomes the same as the one proposed by von Kármán in reference 10. This fact can be proved mathematically by a procedure completely analogous to the one used in appendix B. On the other hand, the use of the convection thickness as defined in equation (15) satisfies the integrated heat-flow equation within the boundary layer, as shown in appendix B. The use of both boundary-layer thicknesses leads to somewhat different results for the local heat-transfer coefficient, and the question arises as to which is preferable. It is pointed out by Schuh in reference 23 that for the purpose of determining heat-transfer coefficients it is more important to satisfy the heat-flow balance, and the use of the convection thickness was therefore recommended. In reference 22, the use of the thermal boundary-layer thickness as defined in equation (16) is investigated, and the results of the calculation with this boundary-layer thickness are found to agree even better with measured values and with other calculations. The convection thickness δ_c and the thermal thickness δ_t for the boundary layer will therefore be used in parallel in the following numerical evaluations.

2447

CALCULATION PROCEDURE

Use of Dimensionless Variables

The procedure which may be followed in determining local heat-transfer coefficients with the relations developed in the preceding section is now explained. Figure 2 shows a sketch of a cylinder with arbitrary cross section and the notation used in the analysis. Before numerical calculations are made, however, it is advisable to change to dimensionless quantities. In order to make this change, the distance x is divided by the major axis L of the cylinder and the mass velocity in the direction of x is divided by an upstream mass velocity. All lengths and mass velocities parallel to y are, in addition, multiplied by the square root of the Reynolds number Re_0 based on the major axis and the upstream mass velocity. The dimensionless variables which are subsequently needed are

$$x^* = \frac{x}{L} \tag{28}$$

$$\delta^* = \frac{\delta}{L}\sqrt{Re_0} \tag{29}$$

$$u_s^* = \frac{\rho_w u_s}{\rho_0 u_{s,0}} \tag{30}$$

$$v_w^* = \frac{\rho_w v_w}{\rho_0 u_{s,0}} \sqrt{Re_0} \tag{31}$$

where

2447

$$Re_0 = \frac{u_{s,0} L \rho_0}{\mu_w} \tag{32}$$

By use of these dimensionless quantities, equation (26) is transformed into

$$\frac{d\delta^*}{dx^*} = \frac{M}{\delta^* u_s^*} \tag{33}$$

where

$$M = \frac{1-m}{2} \eta_b^2 = M\left(\frac{du_s^*}{dx^*} \delta^{*2},\ v_w^* \delta^*\right) \tag{34}$$

according to equations (24) and (25), which, in dimensionless values, are

$$\eta_b^2 m = \frac{du_s^*}{dx^*} \delta^{*2}$$

and

$$-\frac{m+1}{2} f_w \eta_b = v_w^* \delta^*$$

Introduction of the dimensionless quantities into equation (27) leads to

$$\frac{Nu}{\sqrt{Re_0}} = \frac{N}{\delta^*} \tag{35}$$

where

$$Nu = \frac{hL}{k_w} \tag{36}$$

and

$$N = \theta_w' \quad \eta_b = N\left(\frac{du_s^*}{dx^*} \delta^{*2},\ v_w^* \delta^*\right) \tag{37}$$

Charts and Calculation Procedure for Prescribed Coolant Flow

Charts have been prepared which present the functions M and N as expressed by equations (34) and (37) in dependence on $(du_s^*/dx^*)\delta^{*2}$ and $v_w^*\delta^*$. When the values presented in reference 25 were considered for the construction of these charts, it was found that in certain cases one of the free-stream boundary conditions was not fulfilled. This same condition had been overlooked by other previous investigators. As a consequence, spot recalculations were made; it was found that the maximum error in $Nu/\sqrt{Re_0}$ resulting from these recalculations was of the order of 6 percent. Consequently, no attempt was made to recalculate the entire field because of the large amount of labor involved. The charts presented herein were constructed from a combination of these recalculations and results presented in reference 25. Even though all recalculations were not made, it is believed that the charts as presented will give results with an accuracy of the order of 2 or 3 percent. In figures 3 and 4, the dimensionless convection thickness of the boundary layer is used; in figures 5 and 6, the dimensionless thermal boundary-layer thickness is used.

At the stagnation point of any blunt-nosed cylindrical body, conditions are the same as those at the stagnation point of a plate normal to the flow. Therefore $m = 1$, but the value of δ^* is unknown. However, there exists at the stagnation point a unique relation $v_w^*\delta^* = F\left[(du_s^*/dx^*)\delta^{*2}\right]$ which may, for instance, be read along the abscissa in figure 3 or in figure 5. Squaring this equation and dividing both sides by $(du_s^*/dx^*)\delta^{*2}$ result in

$$\frac{v_w^{*\,2}}{\dfrac{du_s^*}{dx^*}} = \frac{1}{\dfrac{du_s^*}{dx^*}\delta^{*2}} F^2\left(\frac{du_s^*}{dx^*}\delta^{*2}\right)$$

These relations are presented in figure 7 for the dimensionless convection boundary-layer thickness and in figure 8 for the dimensionless thermal boundary-layer thickness.

By use of these charts, the calculations for any profile can be made in a very simple manner for either the dimensionless convection or the dimensionless thermal boundary-layer thickness. The method of solution for the convection thicknesses is described subsequently. For the thermal thickness, the procedure is the same.

The values of u_s and du_s/dx must be found for the cylinder profile under consideration either by measurement or by a solution of the inviscid-flow equations. The coolant velocity v_w is prescribed by the porosity of the wall and by the pressure distribution around the profile. From these terms, the values of u_s^*, du_s^*/dx^*, and v_w^* can be calculated. The value of δ_c^* at the stagnation point can be determined

from figure 7 in the following way: The value of $\frac{v_w^{*2}}{du_s^*/dx^*}$ is computed, and the corresponding value of $(du_s^*/dx^*)\ \delta_c^{*2}$ is read from figure 7. A simple algebraic operation then yields the desired value of δ_c^* at the stagnation point.

The dimensionless convection boundary-layer thickness δ_c^* along the cylindrical surface is determined from equation (33); for the numerical evaluation presented herein, this equation was solved by the method of isoclines with the aid of figure 3, depending upon which ratio of stream to wall temperature applied. Equation (33) determines the direction of the tangents to the different δ_c^*-curves which satisfy the equation. The task is to find that curve which contains the δ_c^*-value previously calculated for the stagnation point. For chosen values of x^* and δ_c^*, values of $(du_s^*/dx^*)\ \delta_c^{*2}$ and $v_w^*\delta_c^*$ are computed and the value of M is read from the appropriate part of figure 3. Equation (33) then gives the slope of the tangent at this selected value of x^* for the assumed δ_c^*. Several values of δ_c^* are used for this x^*. The same calculations are repeated for other values of x^*. If the distance between these x^*-values is chosen small enough, an accurate curve of δ_c^* against x^* can be drawn which starts at the desired previously calculated value of δ_c^* at the stagnation point and which will have the correct slope at each value of x^* considered. Figure 9 illustrates this method of solution. Values of N can then be obtained for each of the correct δ_c^*-values and the considered v_w^*-value for each x^* from figure 4 after $(du_s^*/dx^*)\ \delta_c^{*2}$ and $v_w^*\delta_c^*$ are computed (the ratio of stream to wall temperature under consideration determines which part of figure 4 should be used). The value of $Nu/\sqrt{Re_0}$ can finally be obtained from equation (35).

The same calculation procedure can be used when the dimensionless thermal boundary-layer thickness is considered. Figure 8 is used for the determination of the value of δ_t^* at the stagnation point; figure 5 is used to determine M; and figure 6 is used to determine N. The particular ratio of stream to wall temperature under consideration determines which parts of these figures apply for the calculation of the values of M and N. Finally, equation (35) gives the desired value of $Nu/\sqrt{Re_0}$.

Charts and Calculation Procedure for Prescribed Wall Temperature

The heat-transfer coefficients determined by the values of $Nu/\sqrt{Re_0}$ can now be used to calculate the surface temperature of the cylinder when the outside stream temperature and the temperature with which the coolant is supplied to the interior of the cylinder are known. For this purpose a heat balance for an element of the wall as shown in figure 10

2447

is set up. The cylindrical volume element considered may have two plane surfaces, one surface (1) coinciding with the outside surface of the cylinder wall and the other (2) apart from the inside surface of the wall by such a distance that it is situated outside the boundary layer present on this side. (The inside surface has to be considered as a surface of a wall to which suction is applied and on which a boundary layer builds up as shown in reference 29.) The mantle surface (3) of the cylinder may be normal to the wall surfaces. Heat is carried by convection with the cooling air through surfaces 1 and 2. The amount per unit time is indicated in figure 10. It is assumed that the coolant is heated up to the wall surface temperature T_w when it leaves the wall. This assumption is usually well fulfilled. Heat will be also transferred by conduction through the fluid layers immediately adjacent to the outside wall surfaces, the amount being $-k_w\left(\frac{\partial T}{\partial y}\right)_w dA$. In addition, heat may be transferred to the outside wall by radiation; it may be $q_r\ dA$. Heat may also flow into the volume element by conduction in the solid material or by transverse flow of the cooling air. The sum of all these individual flows may be $q_c\ dA$. Then the heat balance is

2447

$$q_r + q_c + c_p\rho_w v_w T_c = c_p\rho_w v_w T_w - k_w\left(\frac{\partial T}{\partial y}\right)_w$$

The heat $-k_w\ (\partial T/\partial y)_w$ transferred per unit area from the gas to the wall was in this report expressed by a heat-transfer coefficient

$$h(T_w - T_s) = -k_w\left(\frac{\partial T}{\partial y}\right)_w$$

Combining these two equations results in

$$q_r + q_c + h(T_s - T_w) = c_p\rho_w v_w(T_w - T_c) \tag{38}$$

This equation permits a calculation of the wall temperature for any place on the cylindrical surface when the coolant velocity v_w is prescribed, when the local radiative heat transfer q_r and the conductive heat flow q_c are known, and when the heat-transfer coefficient h has been obtained. The conductive heat flow q_c is usually small and can be neglected. Such a calculation results in a wall surface temperature which generally will vary along the circumference of the cylinder. When the variations are large, the temperature distribution obtained can be regarded only as an approximation, since the wedge solutions (references 22 and 25) on which the method in this paper is based were obtained for the case of a constant wall temperature.

Usually, however, the problem which faces the designer in an application is somewhat different from the one treated. The purpose of

transpiration cooling is mostly to keep the wall temperature of some structural element below the limits which the material can withstand. On the other hand, the amount of coolant almost always must be kept small, which means that local overcooling should be avoided. For the wall surface under these conditions, a temperature is prescribed which should be uniform about the circumference of the cylinder and the problem is to find that distribution of the coolant velocity v_w which results in the desired wall temperature. Generally, such an investigation requires a trial-and-error procedure which is very involved. The procedure becomes simple and straightforward, however, when the radiative heat flow q_r and the conductive heat flow q_c can be neglected. Such a solution then is useful also as a starting point for the trial-and-error procedure for the case when radiation is present. 2447

The heat balance (equation (38)) can be transformed to

$$\frac{h}{c_p \rho_s u_{s,0}} = \frac{\rho_w v_w}{\rho_s u_{s,0}} \frac{T_w - T_c}{T_s - T_w} \tag{39}$$

when $q_r = q_c = 0$. The ratio of temperature differences in this equation is now a prescribed value. A similar ratio $(T_s - T_w)/(T_s - T_c)$ often appears in turbine-cooling work and is denoted by φ. Introduction of this value and conversion to dimensionless values results in

$$\frac{Nu}{\sqrt{Re_0}} = v_w^* \, Pr \, \frac{1-\varphi}{\varphi} \tag{40}$$

Another expression for $Nu/\sqrt{Re_0}$ is given by equation (35). Combining both equations gives

$$N = v_w^* \delta^* \, Pr \, \frac{1-\varphi}{\varphi} \tag{41}$$

This equation expresses a relation between the parameters N and $v_w^* \delta^*$ in figures 4 and 6 which may be used to insert lines of constant φ into these figures. With the use of these lines the calculation procedure for any specific problem becomes quite simple. The procedure will be described for $T_s/T_w = 1$ (or near 1) and with the use of the convection boundary-layer thickness δ_c. The prescribed temperatures fix the value of φ.

At the stagnation point, $m = 1$ and du_s^*/dx^* is known. In figure 4(a) the intersection between the line $m = 1$ and the line for the prescribed φ determines $v_w^* \delta_c^*$ and $(du_s^*/dx^*) \, \delta_c^{*2}$ and from both values, δ_c^* and v_w^* may be calculated.

The method of isoclines may again be used to determine the development of the boundary layer along the cylindrical surface. The use of this method implies that the gradient $d\delta_c^*/dx^*$ has to be determined for any pair of values x^* and δ_c^*. For an assumed δ_c^*, the value $v_w^*\delta_c^*$ can be found in figure 4(a) as the value on the prescribed φ-curve above the known abscissa value $(du_s^*/dx^*)\ \delta_c^{*2}$. Figure 3(a) then gives M and equation (33), the gradient $d\delta_c^*/dx^*$. A plot similar to figure 9 determines the boundary-layer thickness, and the values v_w^* belonging to these boundary-layer thicknesses represent the coolant-flow distribution for the particular temperature-difference ratio φ.

NUMERICAL EVALUATIONS AND COMPARISONS WITH KNOWN RESULTS

Solid Surfaces

The results of the outlined procedure to calculate local heat-transfer coefficients have to be compared with experimental results or calculations by some other method in order to check the accuracy. The only cylindrical shape for which experimental data or solutions of the boundary-layer equations suitable for such a comparison are available seems to be the cylinder with a circular cross section. Accordingly, local heat-transfer coefficients were calculated by the method proposed in this report with the use of the dimenionless thermal boundary-layer thickness as well as of the dimensionless convection boundary-layer thickness. The results of these calculations are plotted in figure 11 over the dimensionless distance from the stagnation point. Also inserted in the figure is a curve representing the average curve through the experimentally determined local heat-transfer coefficients mentioned in reference 30. It was shown in reference 22 that the measurements correlated well into a single curve when the experiments with very high Reynolds numbers near the critical value for transition to turbulence within the boundary layer were excluded. The tests with high Reynolds numbers gave values of $Nu/\sqrt{Re_0}$ which over the whole upstream side of the cylinder were about 10 percent higher than the ones for the lower Reynolds numbers. The same behavior was found in references 31 and 32 in which it is shown that an increase up to 50 percent in the heat-transfer coefficients over the expected laminar values was caused by the turbulence level in the wind tunnels used. The result of a solution of the boundary-layer equation as presented in reference 1 is also included in figure 11. This method solves the boundary-layer equations and obtains results as a series in the distance along the surface. Also inserted are values obtained by use of the Pohlhausen flat-plate solution when the free-stream velocity is based on the local values and results obtained by the methods of references 12 and 13. Heat-transfer coefficients on wedges with the same local stream velocity and velocity gradient at the same distance from the stagnation point are also included (reference 8). Appendix C explains how these wedge solutions were obtained.

On a cylinder with a circular cross section, separation occurs in the subcritical range near the value $x^* = 0.7$. The stream velocity distribution around the surface of the cylinder which was needed for the calculations was obtained from pressure distributions given in reference 30 and is contained in reference 22.

It may be seen from figure 11 that the use of flat-plate values results in heat-transfer coefficients which are considerably lower than experimental values, whereas the methods in references 12 and 13 result in values which are too high. Much better agreement is found between the wedge heat-transfer coefficients and the experimental results, especially near the stagnation point. Farther downstream, the accuracy is improved by the method of this report. For the largest distance from the stagnation point, the use of the dimensionless thermal boundary-layer thickness results in values which are higher and the use of the dimensionless convection thickness, in values which are lower than the experimental ones. The values calculated by Frössling's solution of the boundary-layer equations are also higher than the experimental ones. Frössling's method has to be considered as an exact solution of the boundary-layer equations. In reference 22 it is recommended, on the basis of the good agreement between Frössling's curve and the values obtained by the use of the thermal boundary-layer thickness, that the method of the equivalent wedge flow be based on the thermal boundary-layer thickness. The values of the heat-transfer coefficients depend primarily on the velocity distribution in the stream around the cross section of the cylinder. The velocity distribution used for the calculation on the circular cylinder is also shown on figure 11. The calculations are made for a Prandtl number of 0.7, for a solid surface ($v_w = 0$) and a temperature ratio T_s/T_w of 1, equivalent to the assumption of constant property values. These calculations agree within 5 percent with the exact calculation and within 8 percent with experiment when the immediate neighborhood of the separation point is excluded. Similar comparisons have already been made in reference 2 for a gas with a Prandtl number of 1 and a different velocity distribution (see fig. 1). This comparison shows that the method proposed by Squire (reference 16) gives heat-transfer coefficients which agree with the exact boundary-layer solution to about the same degree as those of the method of the equivalent wedge flow. The same fact holds for the method indicated in references 15 and 17 especially with the improvement given in reference 4. It can be stated in summary, therefore, that a number of methods exist today which at least for the circular cylinder permit the determination of heat-transfer coefficients on solid surfaces in the laminar region of a gas having constant property values with a very good accuracy. The advantage of the equivalent wedge flow method over those methods just discussed is that it gives solutions in a very short time and that it can be readily extended to include variable property values and transpiration cooling, as was done in this report. The wedge solution, according to reference 7, is still more rapid; however, the results differ from the experimental values up to 15 percent.

2447

Figure 12 gives the analogous results for an elliptic cylinder with the axis ratio 1:2. It may be observed that heat-transfer coefficients on wedges differ only slightly from those obtained for equivalent wedge-type flow, whereas the flat-plate values and the ones calculated with references 12 and 13 are considerably different. No experimental results nor solutions of the boundary-layer equations for a cylinder with such a cross section which could be compared with the approximate solutions are known to the authors. A calculation with Kroujiline's method presented in reference 22 agrees well with the solutions obtained with the equivalent wedge-type flow method. Separation of the flow occurs on such a profile near $x^* = 0.8$. The stream velocities used are calculated values contained in reference 22.

2447

The agreement between the wedge solutions and the results obtained by the method herein is still closer for the elliptic cylinder with axis ratio 1:4 as can be seen from figure 13. The reason for this fact is the type of stream velocity variation occurring on elliptic cylinders. Flow separation occurs on this cylinder near $x^* = 0.85$. The curves in figures 12 and 13 show that the stream velocity is comparatively constant over a considerable part of its circumference after a steep increase near the stagnation point. This behavior is the more pronounced for an axis ratio of 1:4 than for one of 1:2. An inspection of figure 13 shows that, apart from the region near the stagnation point, even the flat-plate values give a reasonably good approximation. Calculations obtained by use of the dimensionless thermal boundary-layer thickness extended to the flow separation point, whereas those for the dimensionless convection boundary-layer thickness did not. It therefore appears advisable to use the dimensionless thermal boundary-layer thickness.

Experimental heat-transfer coefficients found at the University of California for an elliptic cylinder with an axis ratio of 1:4 (reference 33) are about 50 percent higher than the theoretical values shown in figure 13. There are several reasons for this discrepancy. The measured stream velocity distribution was different from the one on which the present calculations are based, probably because of a limited width of the wind tunnel. The cylinder in the experimental investigation was heated by an electric resistance which produced a constant heat flow through the surface per unit area. Accordingly, the surface temperature varied along the circumference of the cylinder, being lowest at the forward stagnation point and increasing in downstream direction. Calculations in reference 33 indicate that the higher values found in the tests are mostly due to this fact. Another increase of the experimental heat-transfer coefficients may again be connected with the turbulence level in the wind tunnel used as discussed in connection with the test results on circular cylinders.

From figures 11 to 13, it may be concluded that, for cylinders with a stream velocity which is fairly constant over the greater part of the circumference, local heat-transfer coefficients may be obtained with good accuracy from wedge solutions. In the region in which the stream velocity variation is considerable, the method of the equivalent wedge flow gives heat-transfer coefficients with an accuracy sufficient for engineering purposes.

Porous Surfaces

2447

Heat-transfer coefficients were calculated by the method of the equivalent wedge flow for cylinders with circular and elliptic cross sections for transpiration-cooled surfaces and different temperature ratios T_s/T_w by using either the thermal or the convection boundary-layer thickness (figs. 14 to 18). The use of both boundary-layer thicknesses gives different results only for large distances from the stagnation point. The variation of the heat-transfer coefficients with the ratio of stream to wall temperature is comparatively small for solid surfaces. This result is in agreement with previous findings. For transpiration-cooled surfaces, however, the effect of the temperature ratio on the heat-transfer coefficients becomes more pronounced, especially on cylinders with nearly circular cross sections. In reference 24 the case of transpiration cooling with small temperature differences is calculated; this reference includes the effect of the temperature ratio by a correction factor which is based on the assumption that this effect is the same as that determined experimentally for impermeable surfaces. A comparison of results shows that the procedure in reference 24 underestimates the effect of temperature ratio for transpiration-cooled surfaces. In addition, it can be observed that transpiration cooling results in a considerable decrease of the heat-transfer coefficients. A larger amount of coolant flow is necessary to reduce the heat-transfer coefficients by the same amounts in regions in which the heat-transfer coefficients are large. Such a region exists at the stagnation point on the cylinder with the axis ratio 1:2, and especially on the cylinder with the axis ratio 1:4.

The variation in coolant flow required to maintain constant wall temperature for transpiration-cooled cylinders with circular and elliptic cross sections is shown in figure 19. The calculations were made for a temperature ratio T_s/T_w of 1, a value of φ of 0.5, and a Prandtl number Pr of 0.7. Figure 19 shows that the highest local coolant-flow rates are necessary near the stagnation point in order to keep the wall temperature down at that place. The magnitude of the coolant-flow rate at the stagnation point is proportional to the square root of the velocity gradient du_s^*/dx^*; this in turn is determined mainly by the value of the radius of curvature at this point. As this

radius of curvature decreases, the required coolant flow increases. This is in agreement with figure 19, which shows that the maximum coolant flow is required at the stagnation point of the elliptic cylinder with the 1:4 axis ratio. Downstream of the stagnation point, the flow rates decrease for each cylinder. Figure 19 also shows that the use of the thermal rather than the convection boundary-layer thickness results in only a very minor increase in coolant flow required to maintain the circular cylinder wall at a constant temperature.

2447

EXTENSION OF CALCULATION TO HIGH-VELOCITY FLOW

The heat generated by internal friction was neglected in equation (5) according to the assumption of small velocities. The equation

$$q = h(T_s - T_w) \tag{42}$$

gives the heat-transfer coefficient for this case. It was already explained that the inclusion of the internal friction for a gas with a Prandtl number of 1 results only in the change that the temperature T in equation (5) and the temperature T_s in equation (42) are now total temperatures, as long as the property values may be regarded constant. The heat-transfer coefficients determined in this report may be used in this case. It was shown in reference 34 with the use of results obtained in reference 35 that the heat-transfer coefficients determined for low-velocity flow apply to high-velocity flow up to a Mach number of about 4 for a gas with a Prandtl number different from 1, when the stream velocity is constant (flat plate) and the heat flow is not too large. The heat-transfer coefficient, however, has now to be defined by the equation

$$q = h(T_{ad} - T_w) \tag{43}$$

in which the temperature T_{ad} denotes the value which an unheated plate assumes in the high-velocity flow. The adiabatic wall temperature may be determined from the recovery factor

$$r_0 = \frac{T_{ad} - T_s}{T_{T,s} - T_s} \tag{44}$$

which was found to be equal to $\sqrt{Pr}$ for laminar flow and for Prandtl numbers not too far from 1. The difference between the total and the static temperatures in the stream is connected with the stream velocity by the equation

$$T_{T,s} - T_s = \frac{u_s^2}{2c_p} \tag{45}$$

For the flat plate with a constant stream velocity, the adiabatic wall temperature is therefore constant.

Conditions are more involved on a cylinder with a stream velocity which varies along its circumference. Even when the recovery factor is assumed to be constant, equations (44) and (45) give an adiabatic wall temperature which varies along the circumference of the cylinder. The fact that the low-velocity heat-transfer coefficients also represented the high-velocity values on a flat plate, however, followed from the fact that the energy equation for constant property values is linear in T, and that a general solution of the nonhomogeneous equation describing the heat transfer including the internal friction could therefore be obtained by superposition of the solution of the homogeneous equation valid for small velocities and a particular solution of the nonhomogeneous equation. Such a superposition results in a constant wall temperature on the flat plate when the solution of the homogeneous equation for constant wall temperature and the one describing the adiabatic wall temperature is used, since the adiabatic wall temperature is also constant. For a cylinder with an arbitrary cross section, however, the adiabatic wall temperature which represents a particular solution of the nonhomogeneous equation varies along the circumference. Therefore, a superposition of this particular solution with the low-velocity solutions for constant wall temperature does not give a constant wall temperature, which was specified for the problems investigated in this report. Accordingly, the heat transfer has now to be calculated with the equation 2447

$$q = h(T_{eff}-T_w) \tag{46}$$

in which T_{eff} has to be determined for constant wall temperature conditions, namely, as the temperature which a particular spot along the surface for which the heat-transfer coefficient is to be determined assumes when the heat flow through the wall at this particular spot is zero and the wall temperature along the circumference of the cylinder is constant.

For flow around wedges, this temperature, which may be referred to as the "effective temperature," can be found from the results in reference 23. It is also determined for several cases in reference 36. The calculation procedure which determines this effective wall temperature from reference 23 is described in appendix D. The calculation shows that this temperature may be again expressed by a recovery factor

$$r_\infty \doteq \frac{T_{eff}-T_s}{T_{T,s}-T_s} \tag{47}$$

The index ∞ is used to indicate that such a recovery factor could be determined experimentally by a model made of a material with a very large heat conductivity so that the internal heat conduction would eliminate all temperature differences along the surface. On the other hand, the recovery factor describing the adiabatic wall temperature in equation (44) has to be determined experimentally by a model made of a material with an infinitely small heat conductivity so as to eliminate internal heat flow. Values for the recovery factor r_∞ determining the effective temperature of a wedge are presented in figure 20. The recovery factors r_0 describing the adiabatic wall temperature according to equation (44) have been calculated for wedges in reference 7. This calculation had resulted in values which decreased slightly with increasing Euler number m. Repetition of these calculations on an electric computing machine, however, according to a communication from Arthur N. Tifford of Ohio State University, showed that the recovery factors for the adiabatic wall temperature are practically independent of the Euler number and have the same values as the recovery factor r_∞ shown in figure 20 for an Euler number m equal to zero.

2447

The consideration up to now dealt with solid surfaces. No information was found in the literature on recovery factors for transpiration-cooled surfaces. Some recovery factors were therefore determined for a transpiration-cooled flat plate and a flow with constant property values (the same for outside and coolant flow) by an integration of the boundary-layer equation (4). The integration was carried out in the same way as in reference 5. The dimensionless stream function f and its second derivative were taken from reference 29. The results of this calculation are presented in figure 21 and the following table where $T_s/T_w = 1$ and $Pr = 0.7$:

f_w	Recovery factor
-1	0.713
-.75	.750
-.50	.786
0	.838
.50	.874
1	.900

The figure shows that the recovery factors decrease considerably with increasing coolant flow. The calculations were extended to positive values of f_w which apply to a surface with suction.

It might be worthwhile to mention that the accurate determination of the adiabatic or effective wall temperature appreciably influences the heat flow as calculated by equation (43) only when the difference $T_{ad}-T_w$ is of the same order of magnitude as or of a small order of magnitude than the difference $T_{T,s}-T_s$ (see also appendix D).

RESULTS AND CONCLUSIONS

An approximate method for the calculation of heat transfer in the laminar region around cylinders of arbitrary cross section was presented. The method, called the equivalent wedge-type flow method, is based on exact solutions of the laminar boundary-layer equations for wedge-type flow and takes into account the influence of large temperature differences between the flow and the cylinder wall and the influence of transpiration cooling. The use of prepared charts reduces calculations to a graphical solution of an ordinary first-order differential equation. The method can be based either on the convection thickness or on the thermal thickness of the boundary layer. The results of calculations based on one thickness differ slightly from those based on the other thickness. There are not enough experimental data available to decide which boundary-layer thickness should be used. Near the separation point, however, the results obtained with the thermal boundary-layer thickness seem somewhat more plausible. 2447

The method was applied to circular and elliptic cylinders. The following results and conclusions are given:

1. Results of experiments and exact calculations were available only for circular cylinders with solid surfaces. Calculations based on the present method and on the thermal boundary-layer thickness agreed within 5 percent with the exact calculation and within 8 percent with experiment when the immediate neighborhood of the separation point was excluded.

2. With the present method, heat-transfer coefficients may be obtained without a knowledge of the flow boundary layer. Consequently, such calculations are more rapid than those based on the momentum and heat-flow equations.

3. Heat-transfer coefficients determined from wedge solutions agreed on the circular cylinder within 15 percent with the results of experiments. The calculation procedure is still more rapid.

4. For elliptic cylinders, the differences between the results of calculations with the various methods decreased as the axis ratio increased from 1:2 to 1:4.

5. The development of the boundary layer is determined by the velocity distribution around the cylinder. The accuracy which has to be expected for the results of calculations with the different methods will therefore depend on the character of the velocity distribution.

6. For cylinders with solid walls, the variation of the heat-transfer coefficients with ratio of stream to wall temperature was comparatively small.

7. For transpiration-cooled surfaces, the effect of temperature ratio on heat-transfer coefficients became pronounced, especially on cylinders with nearly circular cross sections.

8. A considerable decrease in heat-transfer coefficients accompanied transpiration cooling.

9. The influence of transpiration cooling on the recovery factor was investigated for a flat plate and constant property values. It was found that the recovery factor decreased considerably with increasing coolant flow.

2447

Lewis Flight Propulsion Laboratory
National Advisory Committee for Aeronautics
Cleveland, Ohio, March 19, 1952

APPENDIX A

SYMBOLS

2447

The following symbols are used in this report:

A dimensionless wall temperature gradient taken from references 22 and 23, $\sqrt{\frac{2}{m+1}}\,\theta'_w$.

C constant

c_p specific heat at constant pressure

F function

f dimensionless stream function, $(\rho_w\psi)/\sqrt{\mu_w\rho_w x u_s}$

h heat-transfer coefficient

k thermal conductivity

L characteristic dimension (major axis of cylinder)

$M = \frac{1-m}{2}\eta_b{}^2 = M\left(\frac{du_s^*}{dx^*}\delta^{*2},\ v_w^*\delta^*\right)$ (see equation (34))

m Euler number, $\frac{-\partial p/\partial x}{\rho_s u_s{}^2/x}$; $u_s = Cx^m$

$N = \theta'_w\eta_b = N\left(\frac{du_s^*}{dx^*}\delta^{*2},\ v_w^*\delta^*\right)$ (see equation (37))

Nu Nusselt number, hL/k_w

Pr Prandtl number, $c_p\mu/k$

p pressure

q heat flow

$\tilde{q}$ approximated heat flow

q_c heat flow by conduction

2447

q_r heat flow by radiation

Re_0 Reynolds number, $u_{s,0}L\rho_0/\mu_w$

r_0 recovery factor defined by $(T_{ad}-T_s)/(T_{T,s}-T_s)$ (equation (44))

r_∞ recovery factor defined by $(T_{eff}-T_s)/(T_{T,s}-T_s)$ (equation (47))

T temperature in boundary layer

T_s temperature in stream

u velocity component along surface

u_s free-stream velocity

u_s^* dimensionless mass velocity in free stream, $\rho_w u_s/\rho_0 u_{s,0}$

v velocity component normal to surface

v^* dimensionless velocity normal to surface, $\frac{\rho_w v}{\rho_0 u_{s,0}}\sqrt{Re_0}$

x distance from stagnation point along surface

x^* dimensionless distance from stagnation point along surface, x/L

y distance normal to surface

z dimensionless boundary-layer coordinate taken from references 22 and 23, $\sqrt{\frac{m+1}{2}}\,\eta$

z_b $\frac{1}{\sqrt{2-\beta}}\frac{\delta_c}{x}\sqrt{\frac{u_s x}{\nu}}$

β pressure gradient parameter, $2m/(m+1)$

δ boundary-layer thickness

δ^* dimensionless boundary-layer thickness, $(\delta/L)\sqrt{Re_0}$

δ_c convection boundary-layer thickness (equation (15))

δ_c^* dimensionless convection boundary-layer thickness, $(\delta_c/L)\sqrt{Re_0}$

δ_d displacement boundary-layer thickness (equation (13))

δ_i momentum boundary-layer thickness (equation (14))

δ_t thermal boundary-layer thickness (equation (16))

δ_t^* dimensionless thermal boundary-layer thickness, $(\delta_t/L)\sqrt{Re_0}$ 2447

η dimensionless boundary-layer coordinate, $y\sqrt{\frac{\rho_w u_s}{\mu_w x}}$

η_b $\delta\sqrt{\frac{\rho_w u_s}{\mu_w \xi}}$

θ dimensionless temperature-difference ratio, $\frac{T-T_w}{T_s-T_w}$

ϑ dimensionless temperature-difference ratio, $\frac{T-T_s}{T_{T,s}-T_s}$

λ dimensionless stream function taken from reference 26, $-\frac{m+1}{2} f_w$

μ absolute viscosity

ν kinematic viscosity, μ/ρ

ξ distance along wedge, taken from references 22 and 23

ρ density

φ dimensionless temperature-difference ratio, $\frac{T_s-T_w}{T_s-T_c}$

ψ stream function

Subscripts:

ad adiabatic

c coolant, when used with T

eff effective

s stream

T total

w wall

0 except when used with r, refers to a fixed point in the stream

Superscripts:

m exponent of distance along surface from stagnation point for stream velocity, $u_s = Cx^m$

2447

' denotes differentiation with respect to η

APPENDIX B

EVALUATION OF HEAT-FLOW EQUATION

The energy equation (5) will be integrated along y throughout the boundary layer under the conditions of small Mach number, constant wall temperature, and constant specific heat

$$c_p \int_0^\infty \left(\rho u \frac{\partial T}{\partial x} + \rho v \frac{\partial T}{\partial y}\right) dy = \int_0^\infty \frac{\partial}{\partial y}\left(k \frac{\partial T}{\partial y}\right) dy$$

2447

The first term on the left side can be transformed by partial differentiation to

$$\rho u \frac{\partial T}{\partial x} = \frac{\partial}{\partial x}(\rho u T) - T \frac{\partial(\rho u)}{\partial x}$$

An analogous transformation of the second term and consideration that the temperature gradient $\partial T/\partial y$ is zero outside the boundary layer (for $y = \infty$) result in

$$\int_0^\infty \frac{\partial}{\partial x}(\rho u T) dy - \int_0^\infty T \frac{\partial(\rho u)}{\partial x} dy + \rho v T \Big|_0^\infty - \int_0^\infty T \frac{\partial(\rho v)}{\partial y} dy = -\frac{k_w}{c_p}\left(\frac{\partial T}{\partial y}\right)_w$$

The second and fourth terms cancel because of the continuity equation (3). In the first term, the sequence of differentiation and integration can be reversed. Introduction of the convection thickness of the boundary layer leads finally to the integrated heat-flow equation.

$$\rho_s \frac{d}{dx}(u_s \delta_c) - \rho_w v_w = \frac{k_w}{c_p}\left(\frac{\partial \theta}{\partial y}\right)_w \tag{B1}$$

It will now be proved that equation (26), used for the method of the equivalent wedge-type flow, is the same as this integrated heat-flow equation when the convection thickness for the boundary layer is used. Equation (B1) may be transformed by partial differentiation of the first term into

$$\rho_s u_s \frac{d\delta_c}{dx} + \rho_s \delta_c \frac{du_s}{dx} - \rho_w v_w = \frac{k_w}{c_p}\left(\frac{\partial \theta}{\partial y}\right)_w \tag{B2}$$

For wedge-type flow, the convection thickness is given by the expression

$$\delta_c = \eta_c\sqrt{\frac{\mu_w x}{\rho_w u_s}} = \eta_c\sqrt{\frac{\mu_w}{\rho_w C}}\, x^{\frac{1-m}{2}} \tag{B3}$$

Differentiation of this equation gives

2447

$$\frac{d\delta_c}{dx} = \frac{1-m}{2}\,\eta_c\sqrt{\frac{\mu_w}{\rho_w C}}\, x^{-\frac{1+m}{2}} = \frac{1-m}{2}\,\eta_c\sqrt{\frac{\mu_w}{\rho_w x u_s}} \tag{B4}$$

Introducing this expression as well as equations (9) and (12) into equation (B2) gives the equation

$$\frac{1+m}{2}\left(\rho_s\eta_c + \rho_w f_w\right) = \frac{\rho_w}{Pr}\,\theta_w' \tag{B5}$$

which interconnects the convection thickness with the dimensionless temperature gradient at the wall. The gradient of the convection thickness may now be determined from the integrated energy equation (B2) when the expressions in this equation are transformed to the new variables

$$\frac{d\delta_c}{dx} = -m\,\eta_c\sqrt{\frac{\mu_w}{\rho_w x u_s}} - \frac{\rho_w}{\rho_s}\,\frac{1+m}{2}\,f_w\sqrt{\frac{\mu_w}{\rho_w x u_s}} + \frac{\rho_w}{\rho_s}\,\frac{1}{Pr}\,\theta_w'\sqrt{\frac{\mu_w}{\rho_w x u_s}}$$

Replacing the nondimensional temperature gradient in this equation by equation (B5) results in

$$\frac{d\delta_c}{dx} = \frac{1-m}{2}\,\eta_c\sqrt{\frac{\mu_w}{\rho_w x u_s}} = \frac{1-m}{2}\,\eta_c^{\,2}\,\frac{\mu_w}{\rho_w \delta_c u_s}$$

which is the same as equation (26).

It can also be proved by a completely analogous calculation that the method of the equivalent wedge-type flow, when it is used to calculate the momentum thickness of the flow boundary layer, satisfies the integrated momentum equation which is obtained from equation (2) by an integration over y in a manner similar to the derivation of equation (B1)

$$\frac{d}{dx}\left(\rho_s u_s^{\,2}\delta_i\right) + \rho_s u_s\,\frac{du_s}{dx}\,\delta_d - \rho_w v_w u_s = \mu_w\left(\frac{\partial u}{\partial y}\right)_w$$

APPENDIX C

DETERMINATION OF WEDGE SOLUTIONS

The wedge solutions which were used as a first approximation in figures 11 to 13 can be obtained very easily with the use of figure 22 reproduced from reference 9. The heat-transfer coefficient has to be determined on a wedge which has the same stream velocity and its gradient at the same distance from the stagnation point as the real profile. The Euler number for this wedge can be found from equation (23). In the dimensionless coordinates it is 2447

$$m = \frac{x\frac{du_s}{dx}}{u_s} = \frac{x^*}{u_s^*}\frac{du_s^*}{dx^*} \tag{C1}$$

The parameter f_w which determines the coolant flow through the porous wall is found from equation (20), which reads, when converted to dimensionless quantities,

$$f_w = -\frac{2}{m+1} v_w^* \sqrt{\frac{x^*}{u_s^*}} \tag{C2}$$

The value $(Nu/\sqrt{Re_0})\sqrt{x^*/u_s^*}$ can be determined from figure 22, and $Nu/\sqrt{Re_0}$ is finally obtained by multiplication by $\sqrt{u_s^*/x^*}$.

When the temperature ratio φ is prescribed, figure 23 reproduced from reference 9 can be used to obtain the parameter f_w for any Euler number m. Equation (C2) then determines the value v_w^* and the distribution of the required coolant flow along the profile.

APPENDIX D

DETERMINATION OF EFFECTIVE WALL TEMPERATURE

It is shown in reference 23 that for high-velocity flow of a fluid with constant property values around a wedge with constant wall temperature, the temperature field can be expressed by the equation

$$T = (T_w - T_{T,s})(1-\theta) + (T_{T,s} - T_s)\,\vartheta + T_s \tag{D1}$$

2447

in which θ represents the nondimensional temperature field for low-velocity flow and ϑ, the nondimensional temperature field for high-velocity flow and a wall temperature equal to the total stream temperature. The heat flow from the wall, obtained by differentiating equation (D1), is

$$q_w = -k\left(\frac{\partial T}{\partial y}\right)_w = k\left[(T_w - T_{T,s})\left(\frac{\partial \theta}{\partial y}\right)_w - (T_{T,s} - T_s)\left(\frac{\partial \vartheta}{\partial y}\right)_w\right] \tag{D2}$$

With the transformations used in reference 23 (see also appendix E)

$$\left.\begin{aligned} z &= \frac{y}{\sqrt{2-\beta}}\sqrt{\frac{u_s}{\nu x}} \\ u_s &= Cx^m \\ \beta &= \frac{2m}{m+1} \end{aligned}\right\} \tag{D3}$$

equation (D2) can be transformed into

$$q_w = \frac{k}{\sqrt{2-\beta}}\sqrt{\frac{u_s}{\nu x}}\left[(T_w - T_{T,s})\left(\frac{d\theta}{dz}\right)_w - (T_{T,s} - T_s)\left(\frac{d\vartheta}{dz}\right)_w\right] \tag{D4}$$

This equation is to be brought into the form

$$q_w = \frac{k}{\sqrt{2-\beta}}\sqrt{\frac{u_s}{\nu x}}\,(T_w - T_{eff})\left(\frac{d\theta}{dz}\right)_w \tag{D5}$$

A comparison of equations (D4) and (D5) gives

$$T_w - T_{eff} = T_w - T_{T,s} - (T_{T,s} - T_s) \frac{\left(\frac{d\vartheta}{dz}\right)_w}{\left(\frac{d\theta}{dz}\right)_w} \tag{D6}$$

2447

from which the difference between the total and effective gas temperatures can be found. The expression

$$\frac{T_{T,s} - T_{eff}}{T_{T,s} - T_s} = 1 - r_\infty = - \frac{\left(\frac{d\vartheta}{dz}\right)_w}{\left(\frac{d\theta}{dz}\right)_w} \tag{D7}$$

defines this temperature difference and the recovery factor for the effective wall temperature. The nondimensional temperature gradients appearing on the right side of this equation are presented in references 23 and 36. In this way, the values in figure 20 have been determined.

To obtain an estimate of the conditions under which the difference between the adiabatic wall temperature and the effective wall temperature may be neglected, the heat flow into the wall will be approximated by the equation

$$\tilde{q}_w = k(T_w - T_{ad})\left(\frac{d\theta}{dy}\right)_w \tag{D8}$$

and the error of such an approximation will be determined. The ratio of the exact heat-flow equation (D2) to the one approximated by equation (D8) is

$$\frac{q_w}{\tilde{q}_w} = \frac{T_w - T_{T,s}}{T_w - T_{ad}} + \frac{T_{T,s} - T_s}{T_w - T_{ad}} (1 - r_\infty)$$

Introducing the recovery factor for the adiabatic wall temperature

$$T_{T,s} - T_{ad} = (1 - r_0)(T_{T,s} - T_s)$$

gives

$$\frac{q_w}{\tilde{q}_w} = 1 - \frac{T_{T,s}-T_s}{T_w-T_{ad}} (r_\infty - r_0)$$

For an Euler number equal to 1, which characterizes flow near a stagnation point and which, according to figure 20, shows a large difference between the recovery factors r_0 and r_∞, the error is smaller than 5 percent when

$$\frac{T_{ad}-T_w}{T_{T,s}-T_s}$$

is larger than 2.5.

APPENDIX E

COMPARISON OF VARIABLES

This appendix gives a comparison of the variables used in references 9 and 25 with the ones used in references 22, 23, and 26. All of these references deal with wedge-type flow

2447

Symbols from references 9 and 25	Symbols from references 22, 23, and 26	Relation among symbols
m (Eu)	β	$\beta = \frac{2m}{m+1}$
f_w	λ	$\lambda = -\frac{m+1}{2} f_w$
η	z	$z = \sqrt{\frac{m+1}{2}}\,\eta$
θ'_w	A	$A = \sqrt{\frac{2}{m+1}}\,\theta'_w$

The values used in this report are related to the ones in the preceding references by the following equations:

$$\eta_b = \frac{\delta}{x}\sqrt{\frac{u_s x}{\nu}}$$

$$z_b = \sqrt{\frac{m+1}{2}}\,\frac{\delta_c}{x}\sqrt{\frac{u_s x}{\nu}} = \frac{1}{\sqrt{2-\beta}}\,\frac{\delta_c}{x}\sqrt{\frac{u_s x}{\nu}}$$

REFERENCES

1. Frössling, Nils: Verdunstung, Wärmeübergang und Geschwindigkeitsverteilung bei Zweidimensionaler und rotationssymmetrischer laminarer Grenzschichtströmung. Lunds Universitates Arsskrift, N.F. Avd. 2, Bd. 36, Nr. 4, 1940, S. 1-31.

2. Goland, Leonard: A Theoretical Investigation of Heat Transfer in the Laminar Flow Regions of Airfoils. Jour. Aero. Sci., vol. 17, no. 7, July 1950, pp. 436-440.

3. Sears, W. R.: The Boundary Layer of Yawed Cylinders. Jour. Aero. Sci., vol. 15, no. 1, Jan. 1948, pp. 49-52.

4. Tifford, Arthur N., and Wolansky, John: On the Calculation of the Rate of Heat Transfer Through a Laminar Boundary Layer. Jour. Aero. Sci., vol. 18, no. 6, June 1951, p. 427.

5. Pohlhausen, E.: Der Wärmeaustausch zwischen festen Körpern und Flüssigkeiten mit kleiner Reibung und Kleiner Wärmeleitung. Z.f.a.M.M., Bd. 1, Heft 2, 1921, S. 115-121.

6. Boelter, L. M. K., Grossman, L. M., Martinelli, R. C., and Morrin, E. H.: An Investigation of Aircraft Heaters. XXIX - Comparison of Several Methods of Calculating Heat Losses from Airfoils. NACA TN 1453, 1948.

7. Eckert, E., and Drewitz, O.: Calculation of the Temperature Field in the Laminar Boundary Layer of an Unheated Body in a High Speed Flow. R.T.P. Trans. No. 1594, M.A.P.

8. Ellerbrock, Herman H., Jr.: Some NACA Investigations of Heat-Transfer Characteristics of Cooled Gas-Turbine Blades. Paper presented at the General Discussion on Heat Transfer. Inst. Mech. Eng. (London) and A.S.M.E. (New York) Conference (London), Sept. 11-13, 1951.

9. Brown, W. Byron: Exact Solution of the Laminar Boundary Layer Equations for a Porous Plate with Variable Fluid Properties and a Pressure Gradient in the Main Stream. Paper presented before the First U. S. National Congress of Applied Mechanics (Chicago), June 11-16, 1951.

10. von Kármán, Th.: On Laminar and Turbulent Friction. NACA TM 1092, 1946.

11. Pohlhausen, K.: Zur näherungsweisen Integration der Differentialgleichung der laminaren Grenzschicht. Z.f.a.M.M., Bd. 1, Heft 4, Aug. 1921, S. 252-268.

12. Frick, Charles W. Jr., and McCullough, George B.: A Method for Determining the Rate of Heat Transfer from a Wing or Streamline Body. NACA Rep. 830, 1945.

13. Allen, H. Julian, and Look, Bonne C.: A Method for Calculating Heat Transfer in the Laminar Flow Region of Bodies. NACA Rep. 764, 1943.

2447

14. Kroujiline, G.: Transmission of Heat Past a Circular Cylinder in a Transverse Current of Fluid. Sci. Abstract, Sec. A-Physics, vol. XXXIV, 1936, no. 4267. (Abstract from Tech. Phys., (U.S.S.R.), vol. 3, no. 4, 1936, pp. 311-320. (In French).)

15. Dienemann, W.: Calculation of the Thermal Boundary Layer of a Body in Incompressible Laminar Flow. Jour. Aero. Sci., vol. 18, no. 1, Jan. 1951, pp. 64-65.

16. Squire, H. B.: Heat Transfer Calculation for Aerofoils. R. & M. No. 1986, British A.R.C., Nov. 1942.

17. Lighthill, M. J.: Contributions to the theory of heat transfer through a laminar boundary layer. Proc. Roy. Soc. (London), ser. A, vol. 202, no. A1070, Aug. 7, 1950, pp. 359-377.

18. Tifford, Arthur N.: On the Theory of Heat Transfer Through a Laminar Boundary Layer. Jour. Aero. Sci., vol. 18, no. 4, April 1951, pp. 283-284.

19. Kalikhman, L. E.: Heat Transmission in the Boundary Layer. NACA TM 1229, 1949.

20. Ginzel, J.: Ein Pohlhausenverfahren zur Berechnung laminarer kompressibler Grenzschichten an einer geheizten Wand. Z.f.a.M.M., Bd. 29, Heft 11/12, Nov./Dez. 1949, S. 21-337.

21. Kuerti, G.: The Laminar Boundary Layer in Compressible Flow. No. 496, Dept. of Eng., Harvard Univ. Publ., 1950-51. (Reprinted from Advances in Appl. Mech., vol. II, 1951, pp. 21-92.)

22. Eckert, E.: Die Berechnung des Wärmeübergangs in der laminaren Grenzschicht umströmter Körper. VDI Forschungsheft 416, Bd. 13, Sept. und Okt., 1942.

23. Schuh, H.: Laminar Heat Transfer in Boundary Layers at High Velocities. Rep. & Trans. 810, British M.A.P., April 15, 1947.

24. Staniforth, R.: Contributions to the Theory of Effusion Cooling of Gas Turbine Blades. Paper presented at the General Discussion on Heat Transfer. Inst. Mech. Eng. (London) and A.S.M.E. (New York) Conference (London), Sept. 11-13, 1951.

25. Brown, W. Byron, and Donoughe, Patrick L.: Tables of Exact Laminar-Boundary-Layer Solutions When the Wall is Porous and Fluid Properties are Variable. NACA TN 2479, 1951.

2447

26. Eckert, E. R. G.: Heat Transfer and Temperature Profiles in Laminar Boundary Layers on a Sweat-Cooled Wall. Tech. Rep. No. 5646, Air Materiel Command, Nov. 3, 1947.

27. Tifford, Arthur N.: Simplified Compressible Laminar Boundary-Layer Theory. Jour. Aero. Sci., vol. 18, no. 5, May 1951, pp. 358-359.

28. Howarth, L.: Concerning the Effect of Compressibility on Laminar Boundary Layers and Their Separation. Proc. Roy. Soc. (London), ser. A, vol. 194, no. A1036, July 28, 1948, pp. 16-42.

29. Schlichting, Hermann, and Bussmann, Karl: Exakte Lösungen für die laminare Grenzschicht mit Absaugung und Ausblasen. Schriften d. D. Akad. Luftfahrtforschung, Bd. 7B, Heft 2, 1943.

30. Schmidt, Ernst, and Wenner, Karl: Heat Transfer over the Circumference of a Heated Cylinder in Transverse Flow. NACA TM 1050, 1943.

31. Giedt, W. H.: Effect of Turbulence Level of Incident Air Stream on Local Heat Transfer and Skin Friction on a Cylinder. Jour. Aero. Sci., vol. 18, no. 11, Nov. 1951, pp. 725-730.

32. Gelder, Thomas F., and Lewis, James P.: Comparison of Heat Transfer from Airfoil in Natural and Simulated Icing Conditions. NACA TN 2480, 1951.

33. Seban, R. A., and Drake, R. M., Jr.: Local Heat Transfer Coefficients on Surface of an Elliptical Cylinder in a High Speed Air Stream. Series no. 41, issue no. 6, Engineering Dept., Univ. of Calif. (Berkeley), Jan. 10, 1952. (USAF-AMC Contract 33(038)-12941.)

34. Eckert, E., and Drewitz, O.: The Heat Transfer to a Plate in Flow at High Speed. NACA TM 1045, 1943.

35. Busemann, A.: Gasströmung mit laminarer Grenzschicht entlang einer Platte. Z.f.a.M.M., Bd. 15, Heft 1-2, Feb. 1935, S. 22-25.

36. Tifford, Arthur N.: Specific Aerodynamic and Propulsion Problems. I. Some Prandtl Number Effects on the Transfer of Heat. Eng. Exp. Station News, The Ohio State Univ., vol. XXII, no. 1, Feb. 1950, p. 11.

2447

2447

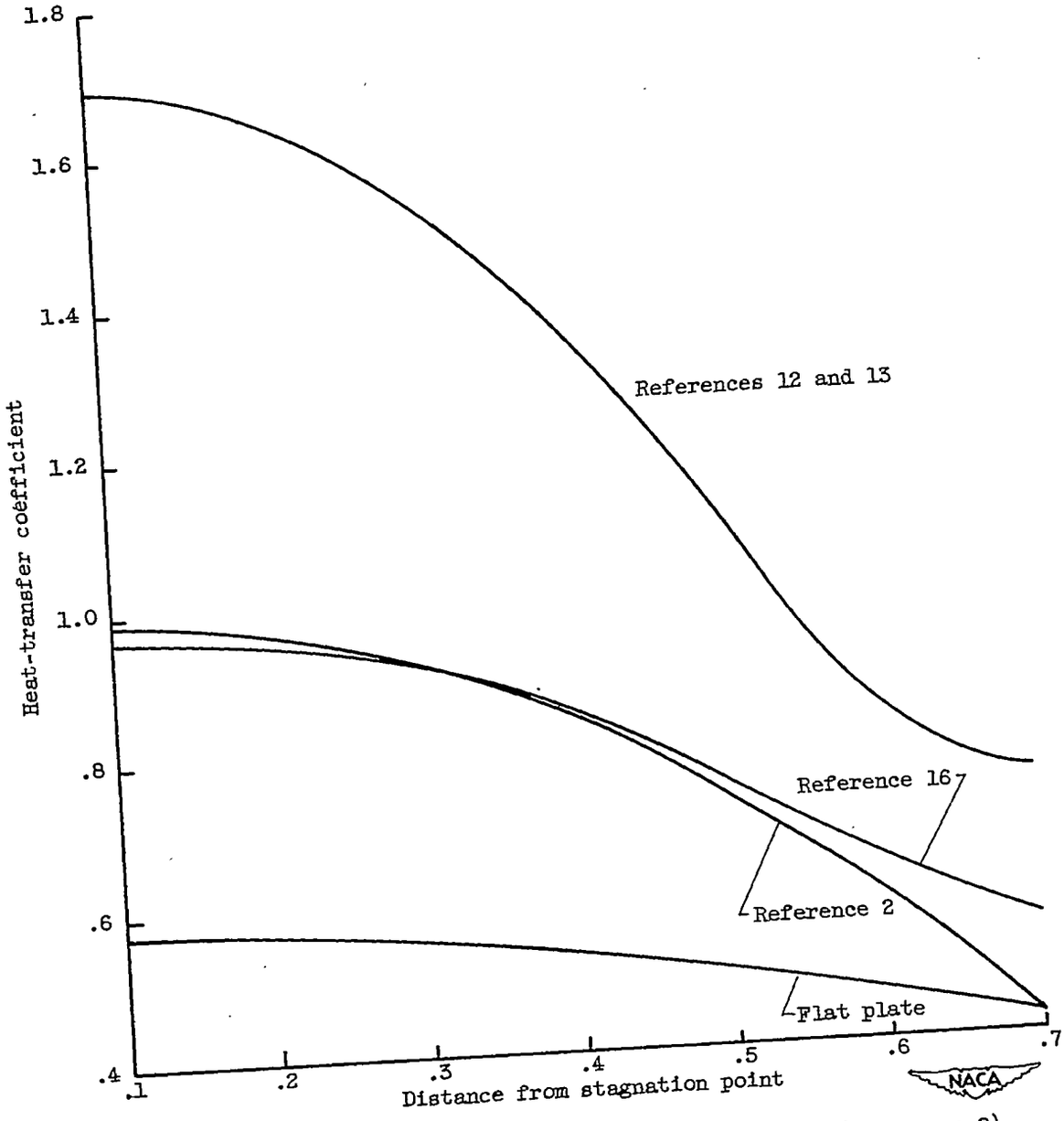

Figure 1. - Heat-transfer coefficient for cylinder (reference 2).

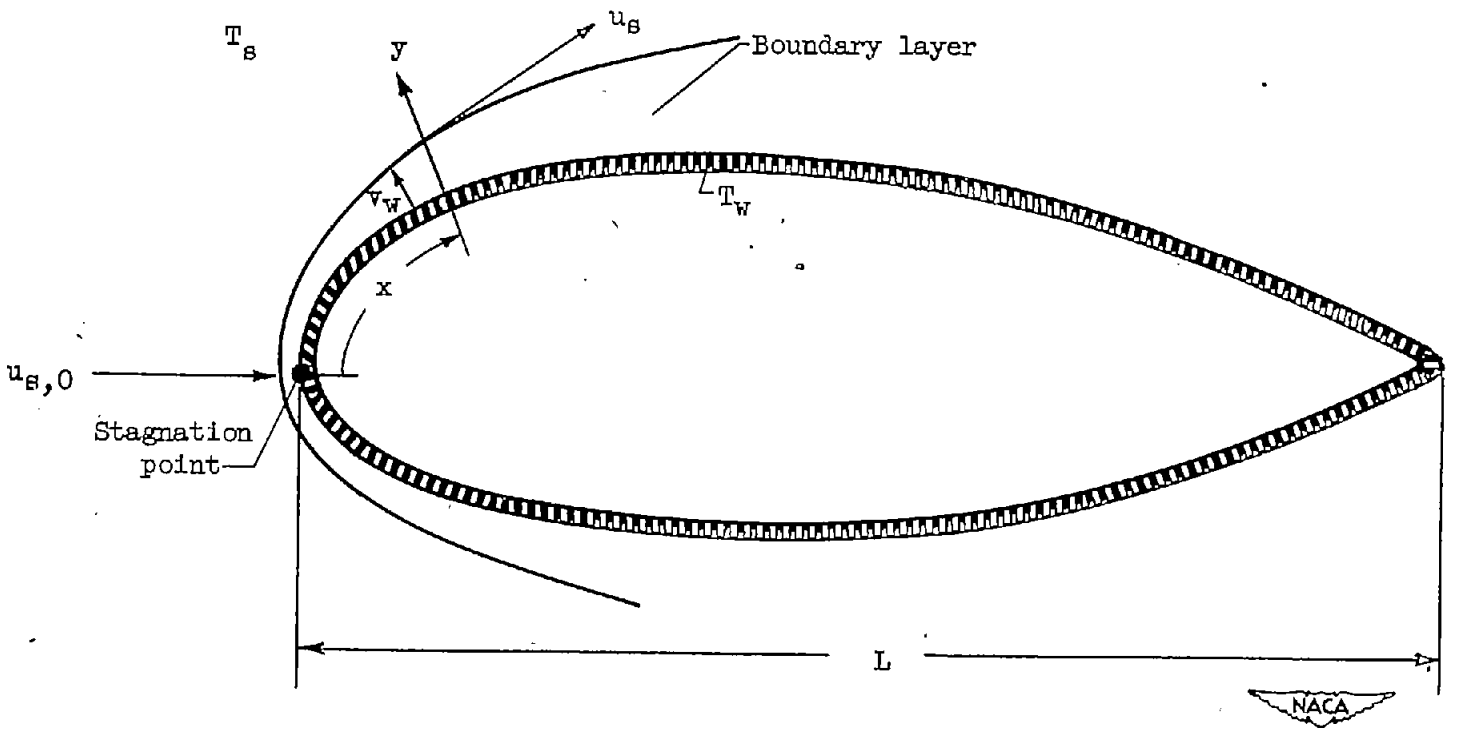

Figure 2. - Sketch of cylinder indicating notation used.

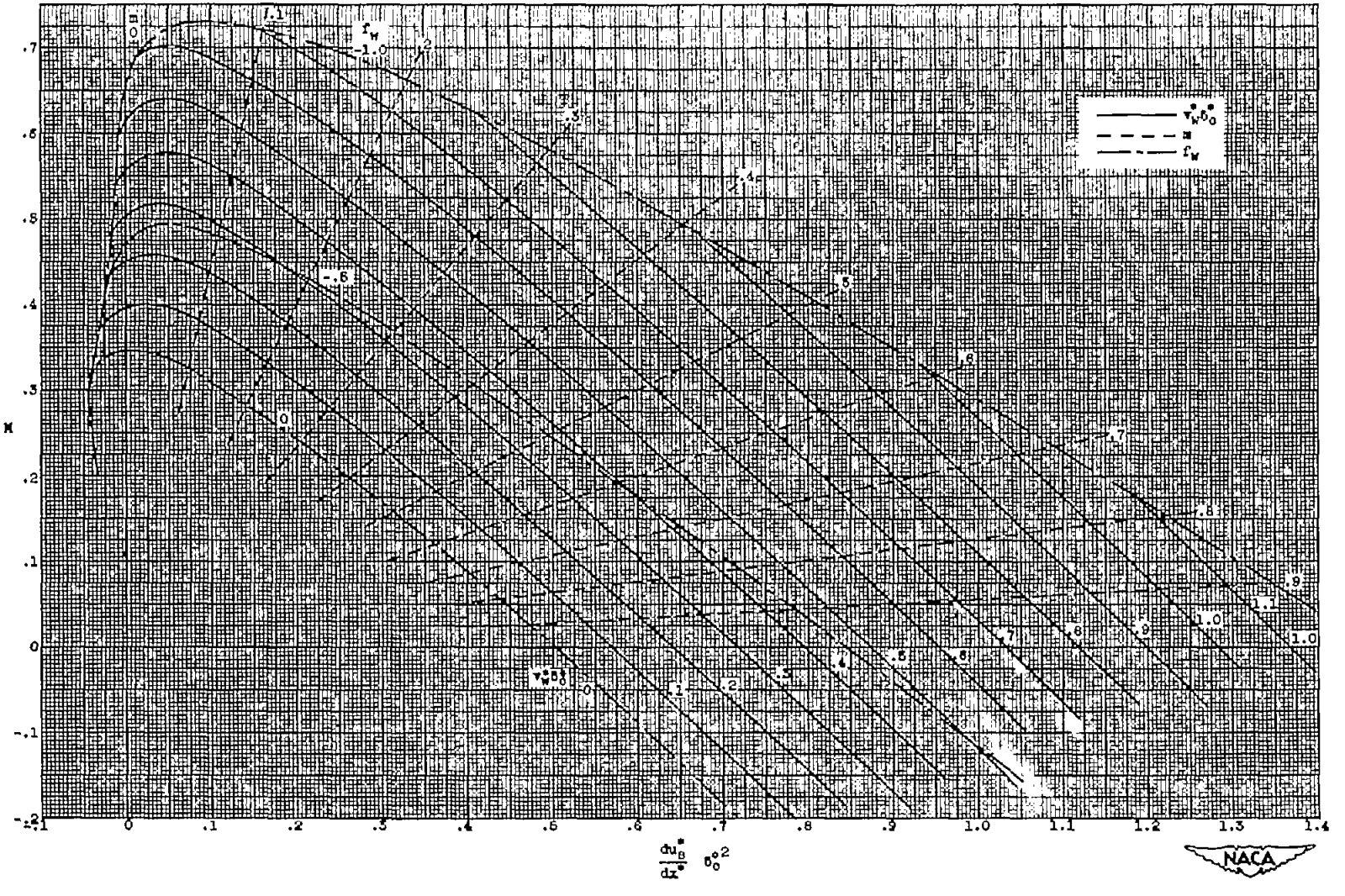

(a) T_e/T_w, 1.

Figure 3. - Chart for use in determination of M for dimensionless convection boundary-layer thickness. Pr, 0.7.

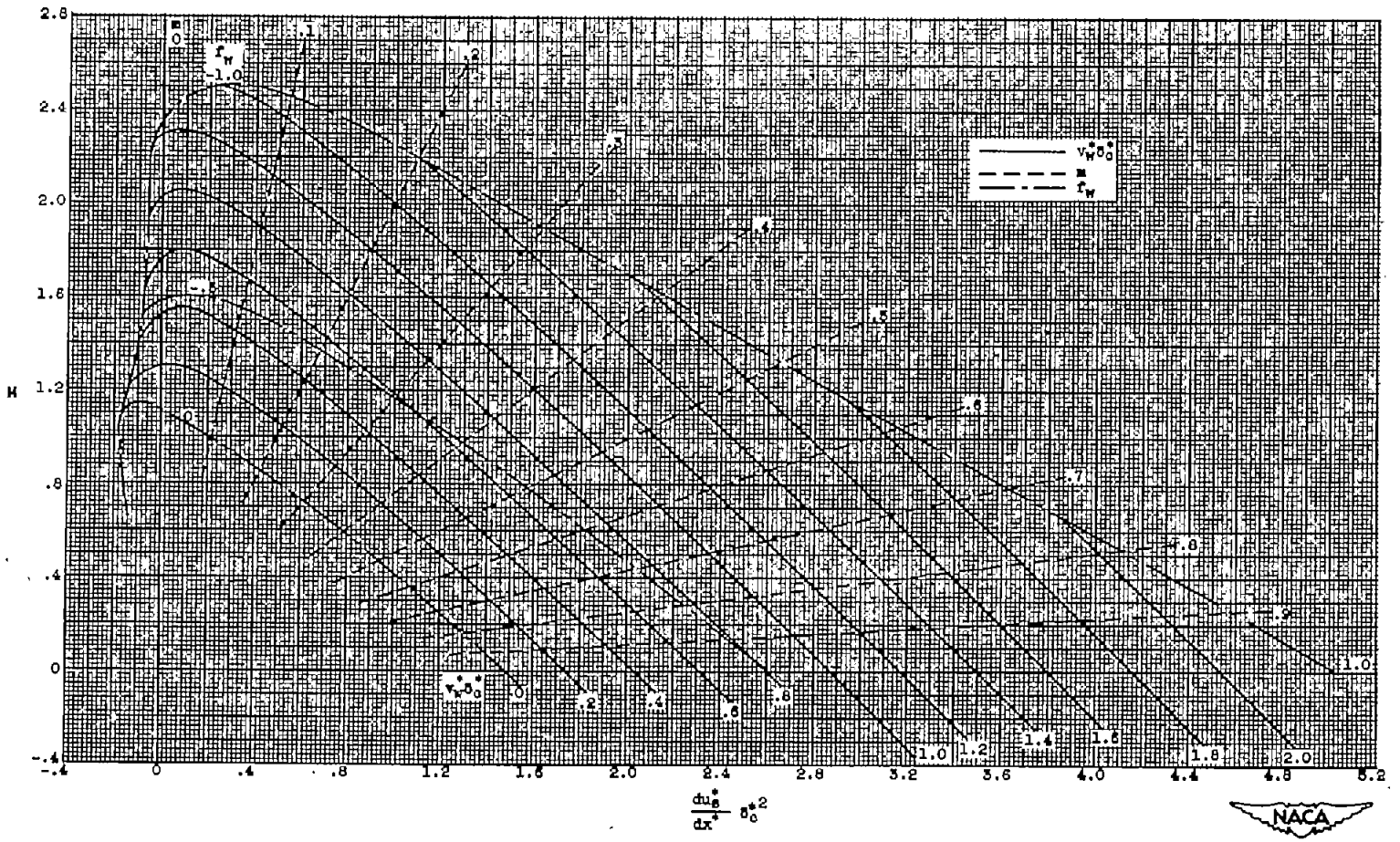

(b) T_B/T_w, 2.

Figure 3. - Continued. Chart for use in determination of M for dimensionless convection boundary-layer thickness. Pr, 0.7.

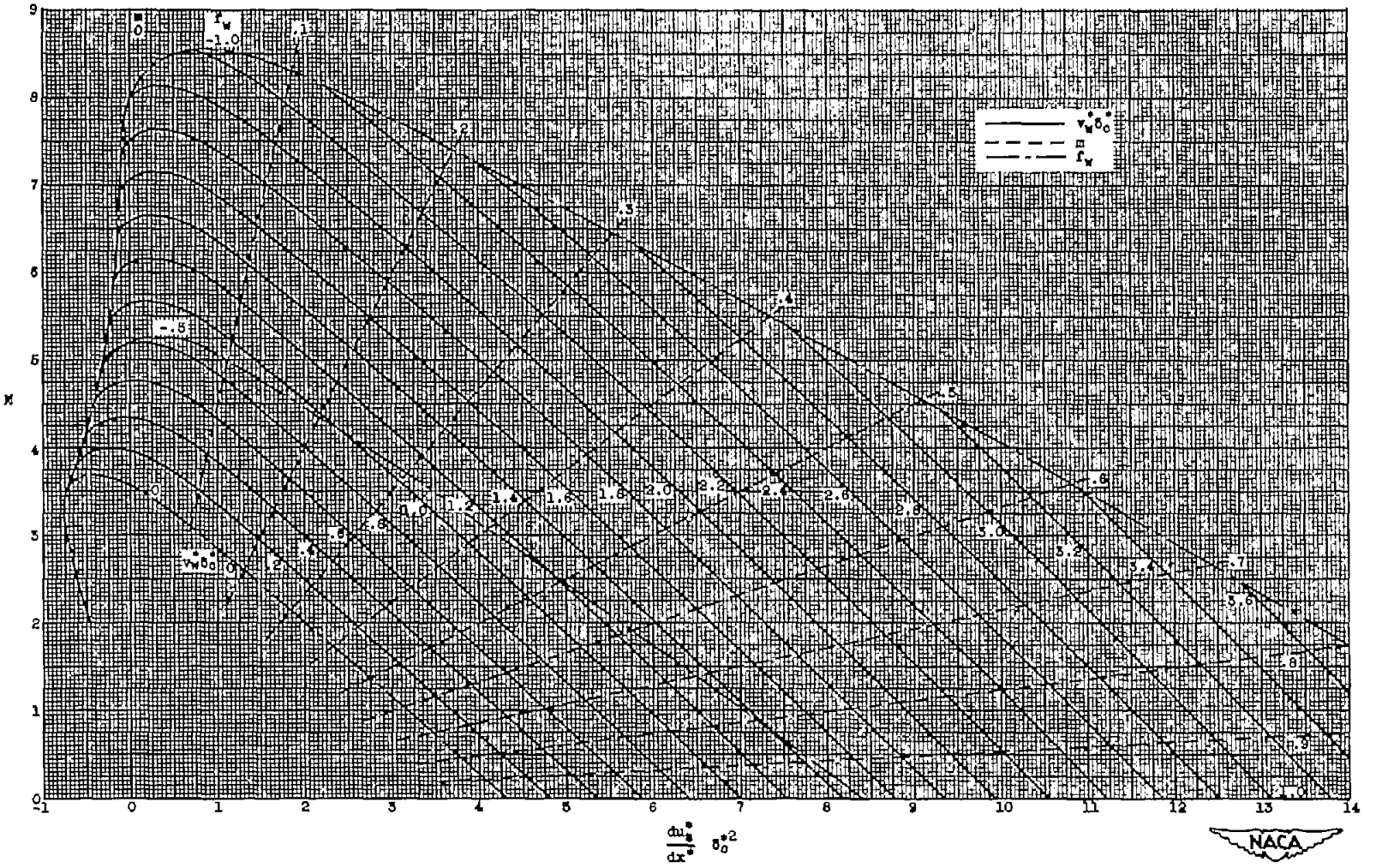

(o) T_a/T_w, 4.

Figure 3. - Concluded. Chart for use in determination of M for dimensionless convection boundary-layer thickness. Pr, 0.7.

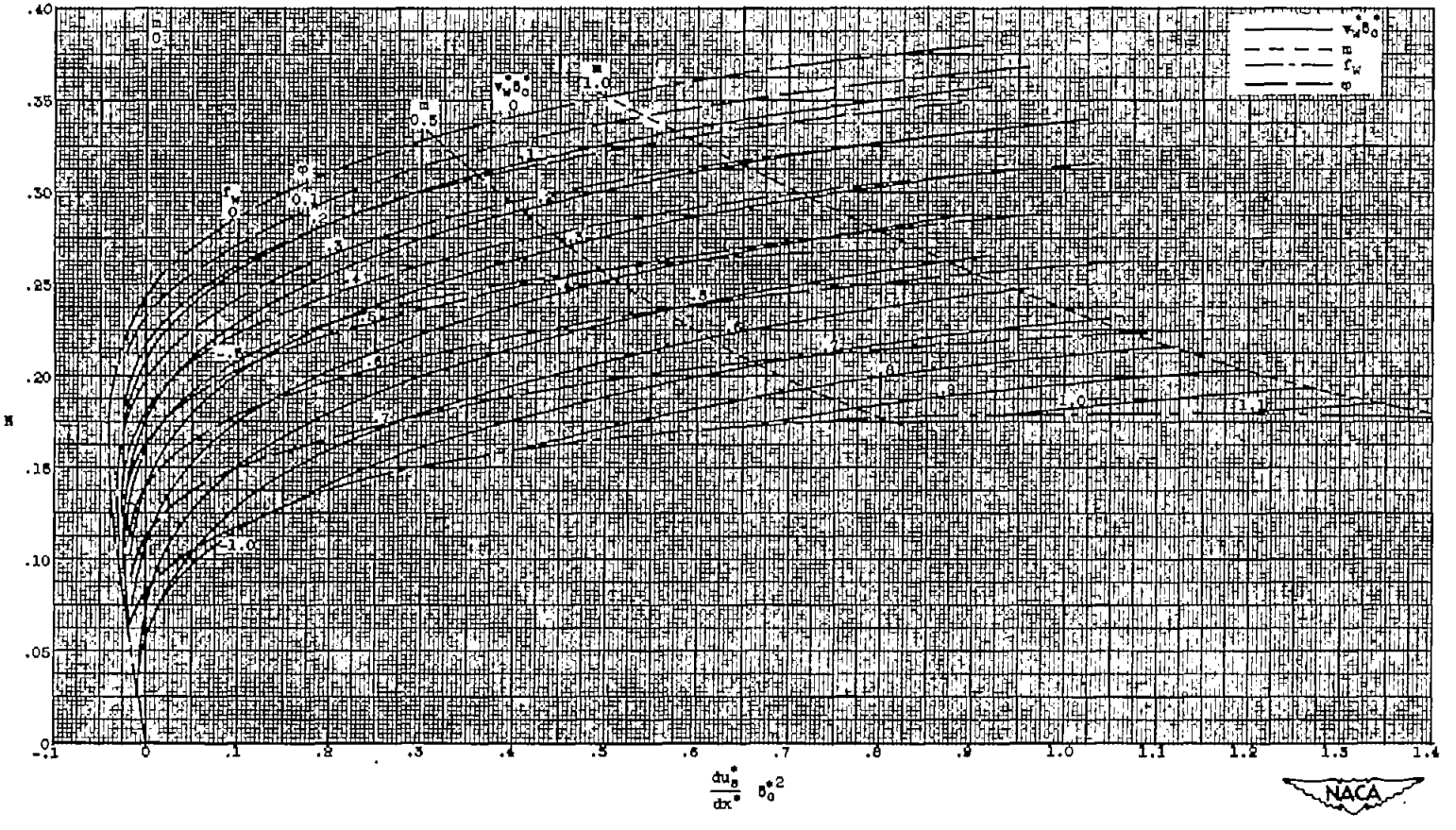

(a) T_s/T_w, 1.

Figure 4. - Chart for use in determination of N for dimensionless convection boundary-layer thickness. Pr, 0.7.

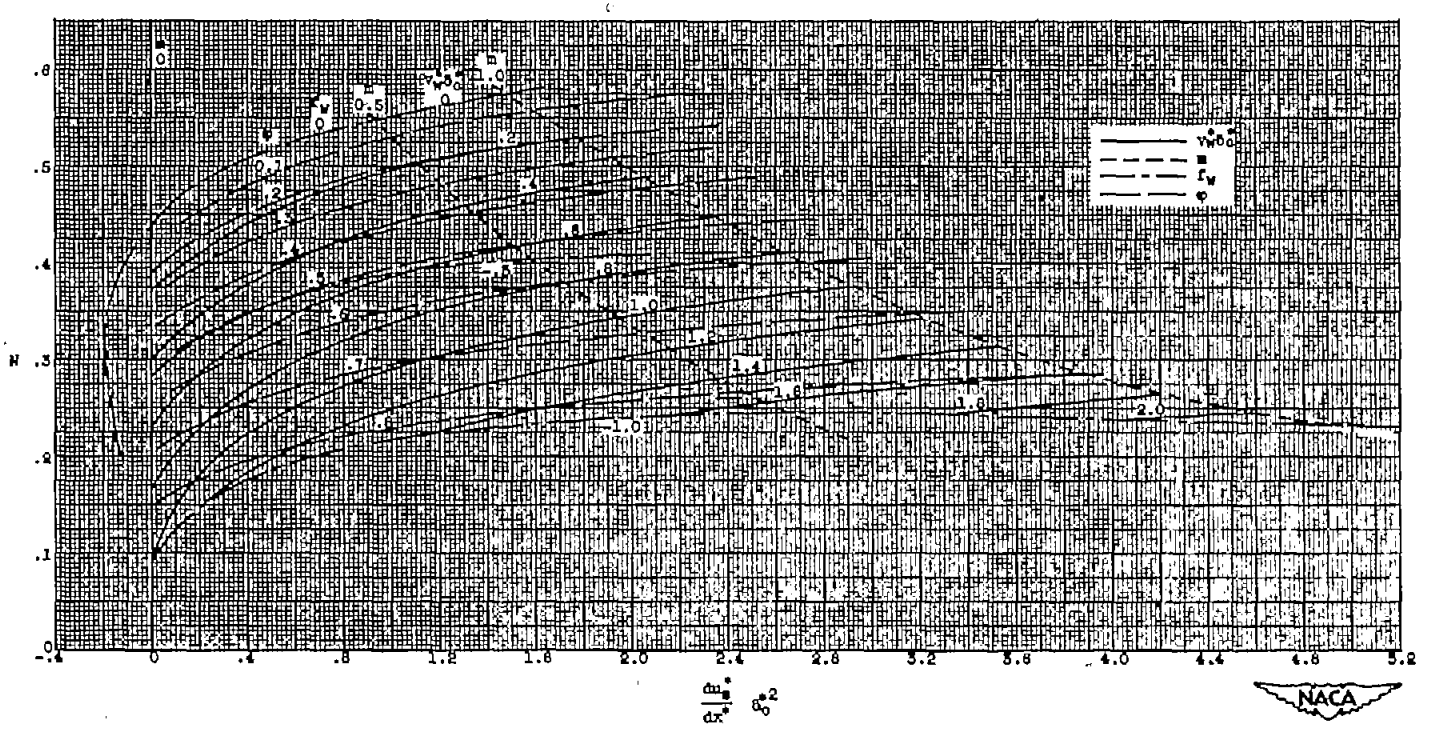

(b) T_B/T_W, 2.

Figure 4. - Continued. Chart for use in determination of N for dimensionless convection boundary-layer thickness, Pr, 0.7.

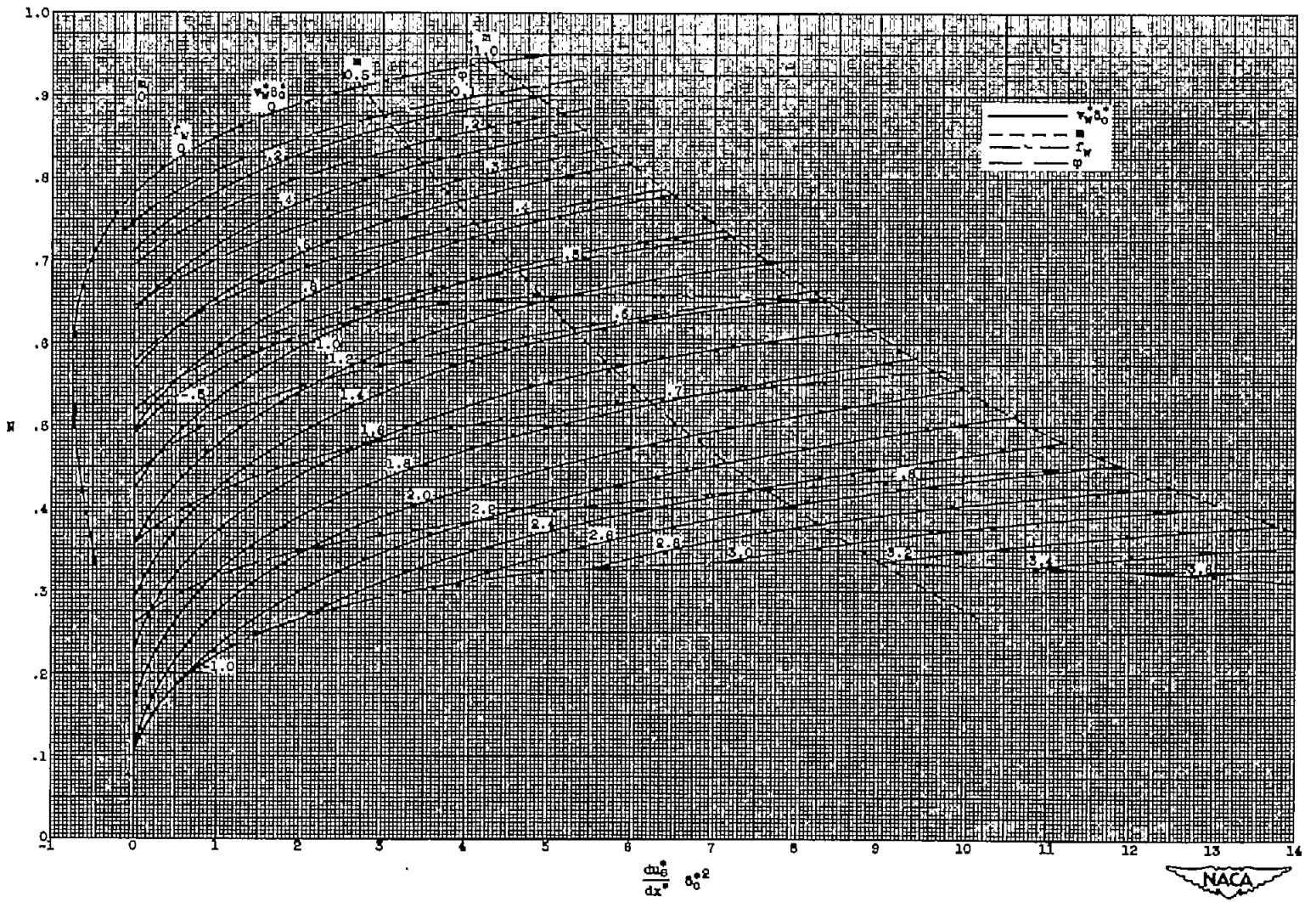

(c) T_B/T_W, 4.

Figure 4. - Concluded. Chart for use in determination of N for dimensionless convection boundary-layer thickness. Pr, 0.7.

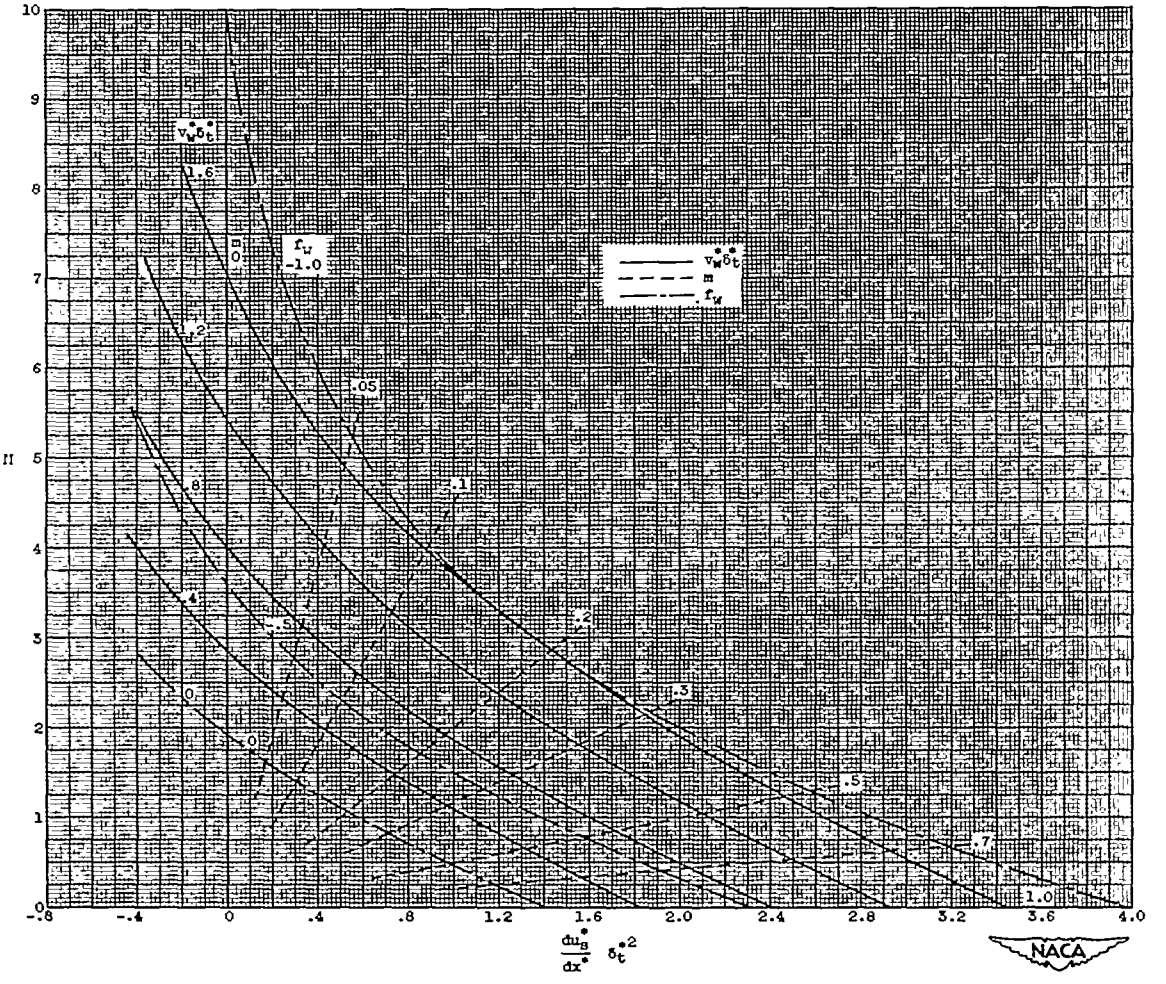

(a) T_B/T_W, 1.

Figure 5. - Chart for use in determination of H for dimensionless thermal boundary-layer thickness. Pr, 0.7.

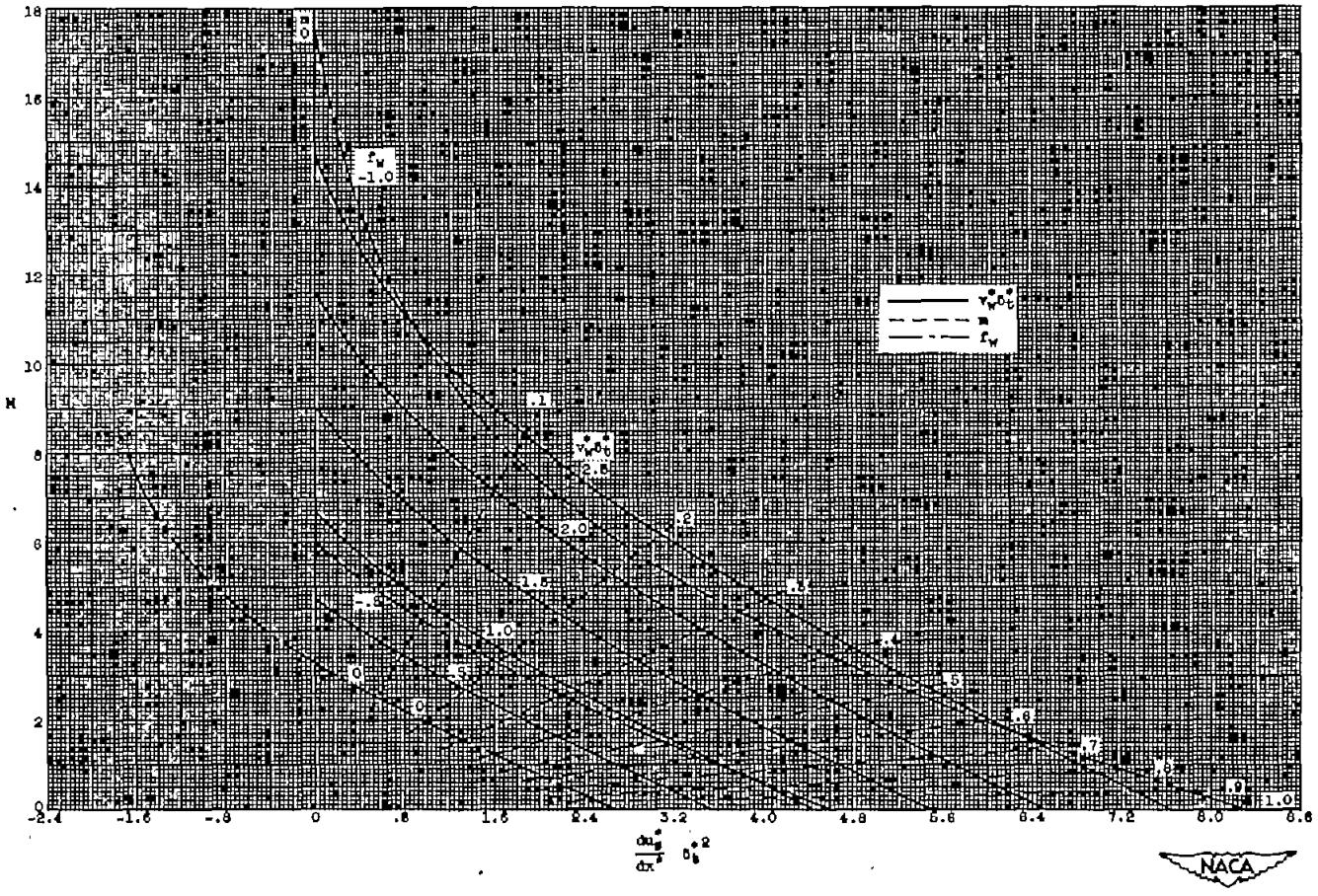

(b) T_s/T_w, 2.

Figure 5. - Continued. Chart for use in determination of M for dimensionless thermal boundary-layer thickness. Pr, 0.7.

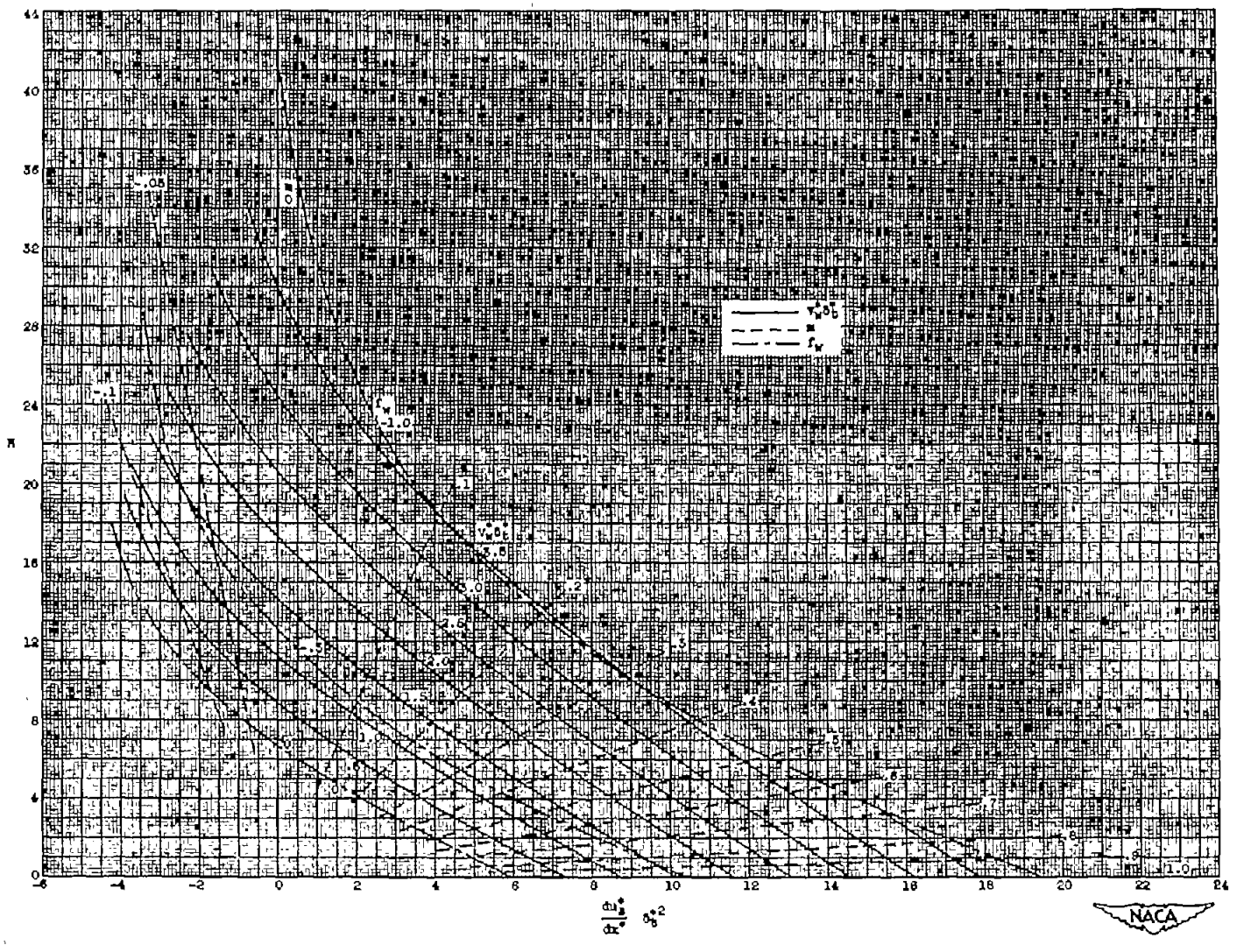

(c) T_0/T_w, 4.

Figure 5. - Concluded. Chart for use in determination of M for dimensionless thermal boundary-layer thickness. Pr, 0.7.

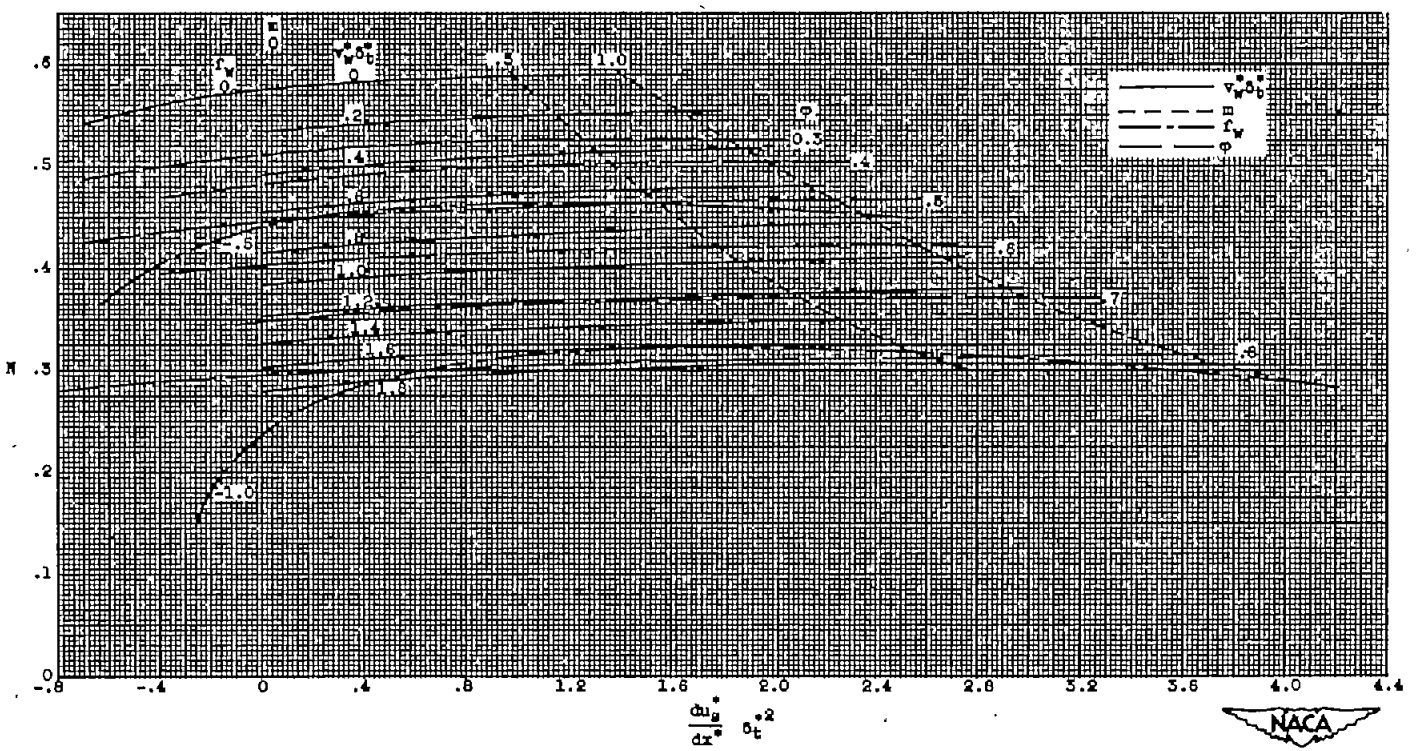

(a) T_s/T_w, 1.

Figure 6. - Chart for use in determination of N for dimensionless thermal boundary-layer thickness. Pr, 0.7.

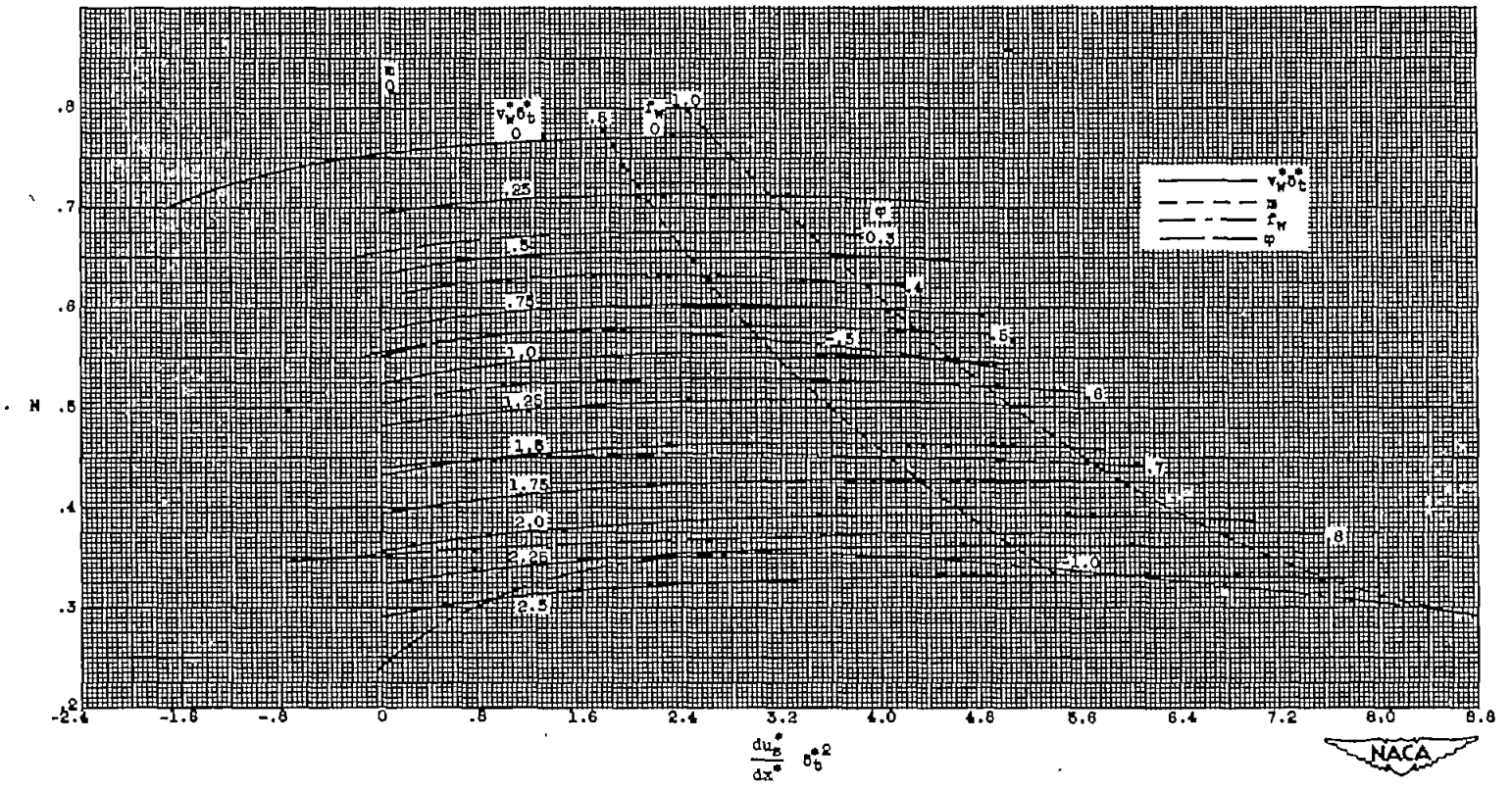

(b) T_e/T_w, 2.

Figure 6. - Continued. Chart for use in determination of H for dimensionless thermal boundary layer thickness. Pr, 0.7

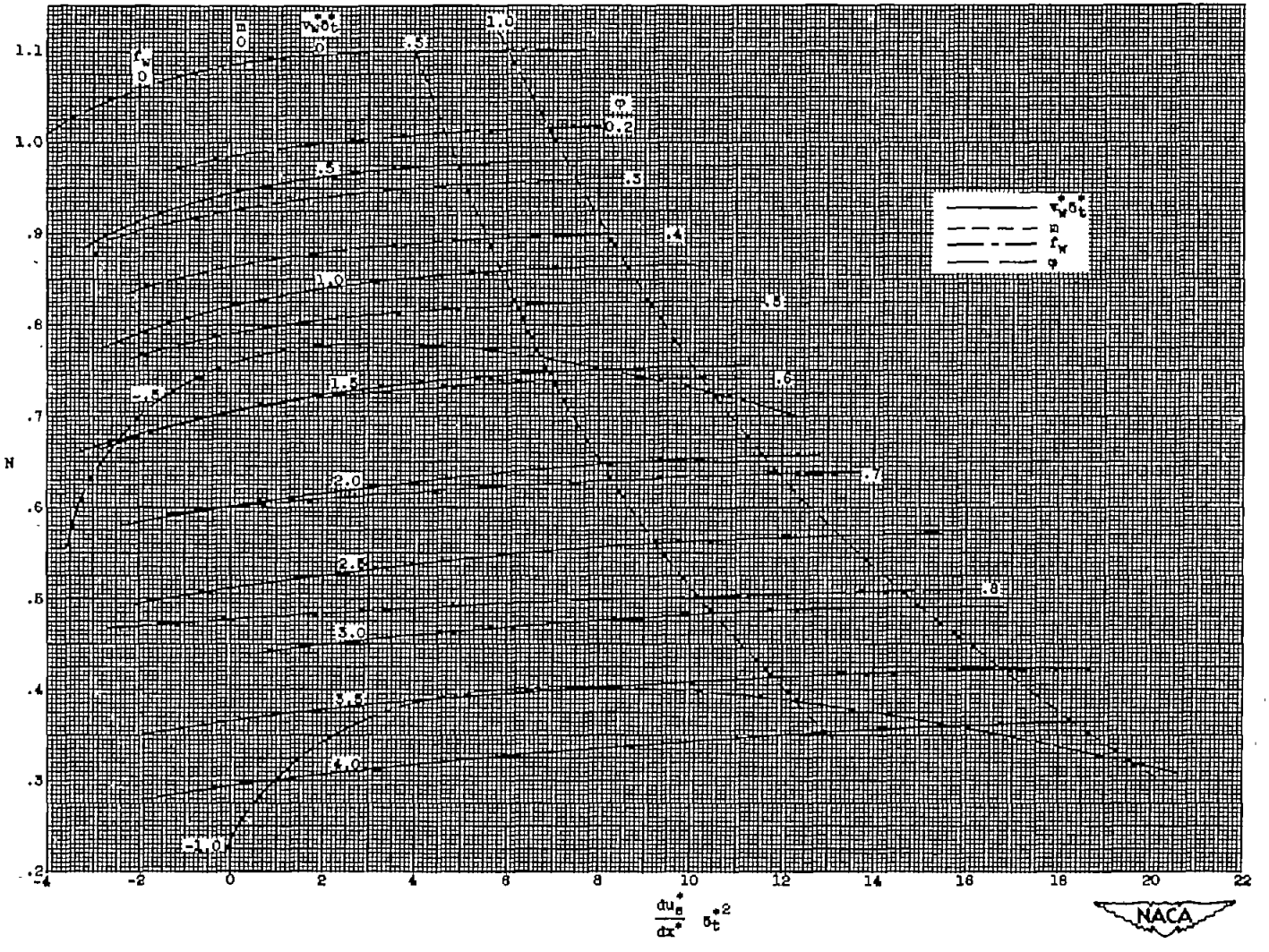

(c) T_e/T_w, 4.

Figure 6. - Concluded. Chart for use in determination of N for dimensionless thermal boundary-layer thickness. Pr, 0.7.

2447

2447

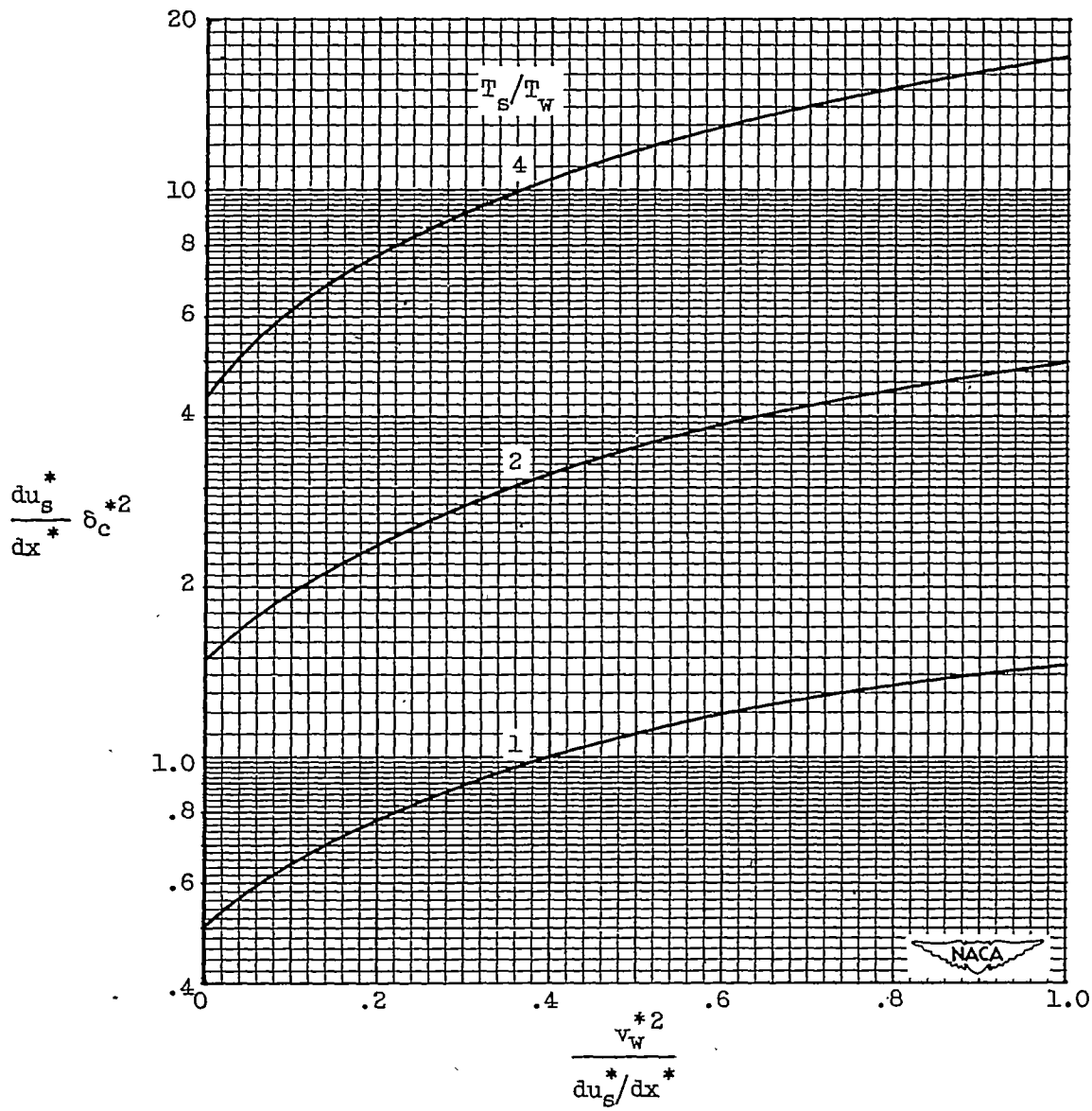

Figure 7. - Chart for use in determination of dimensionless convection boundary-layer thickness at stagnation point.

2447

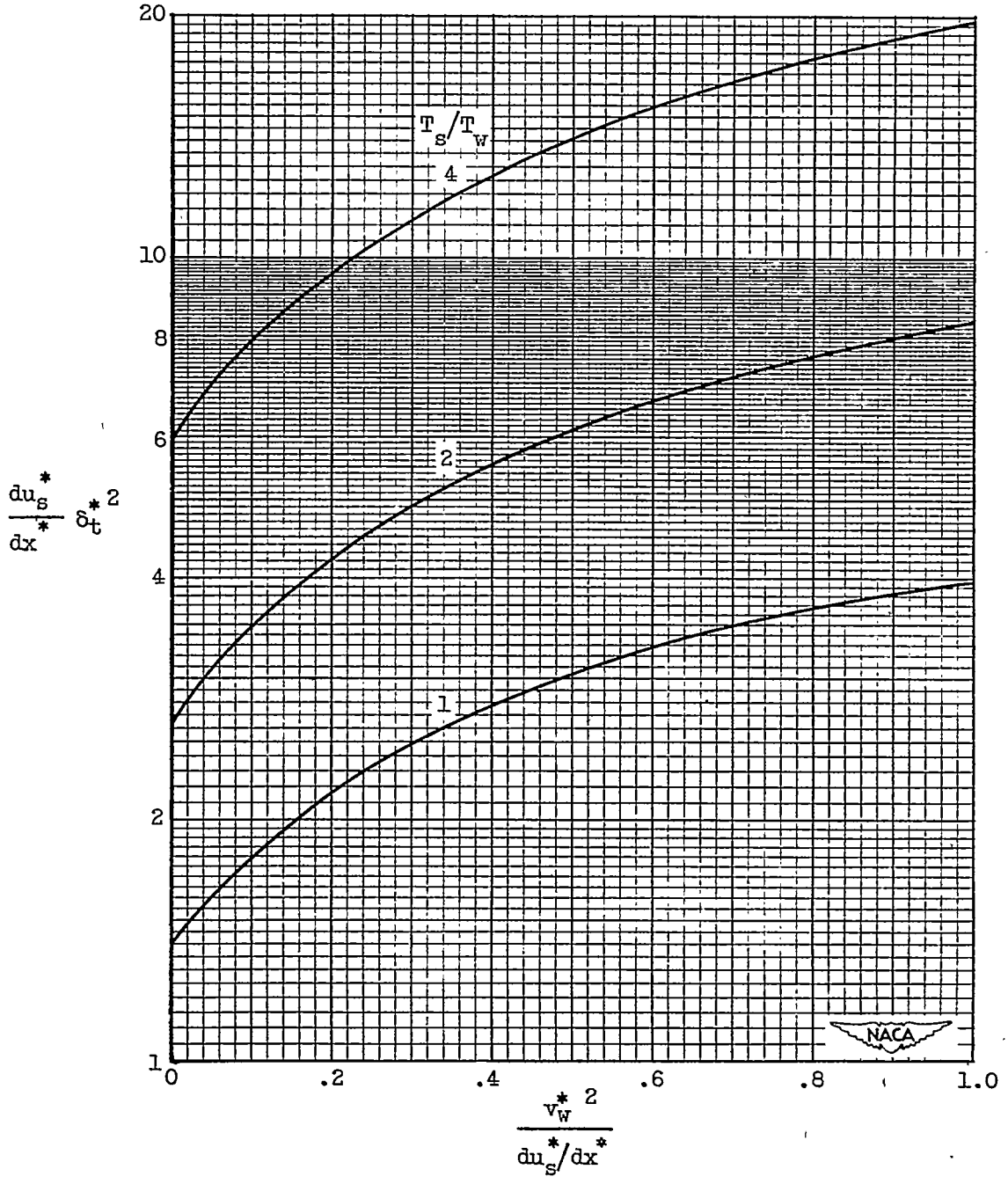

Figure 8. - Chart for use in determination of dimensionless thermal boundary-layer thickness at stagnation point.

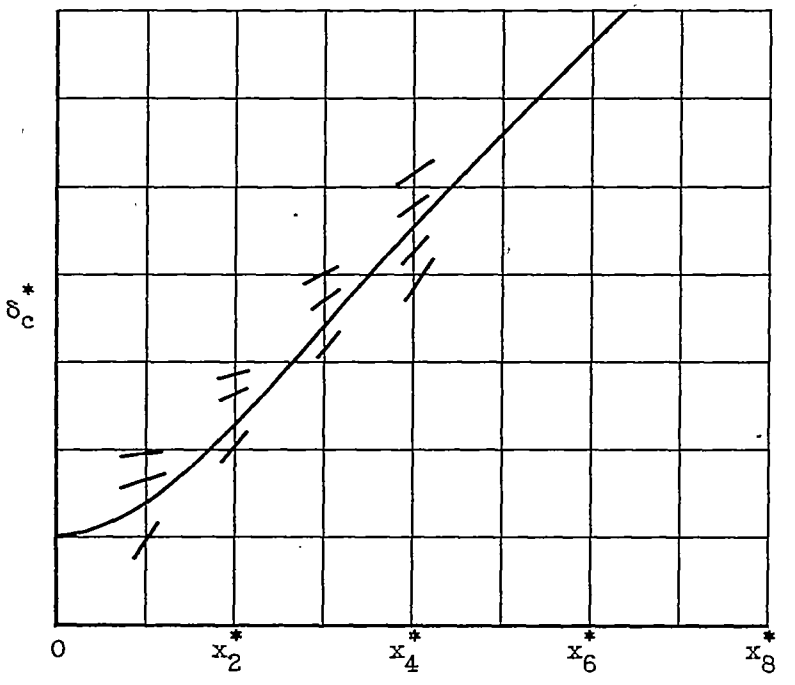

Figure 9. - Isocline solution of boundary-layer equation.

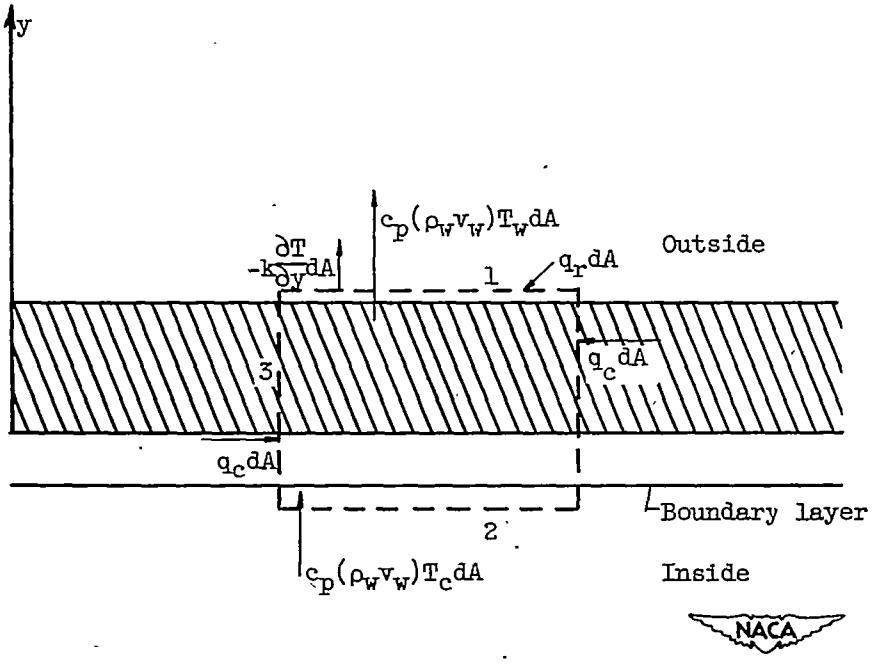

Figure 10. - Cross section through part of cylinder wall used in setting up heat balance.

2447

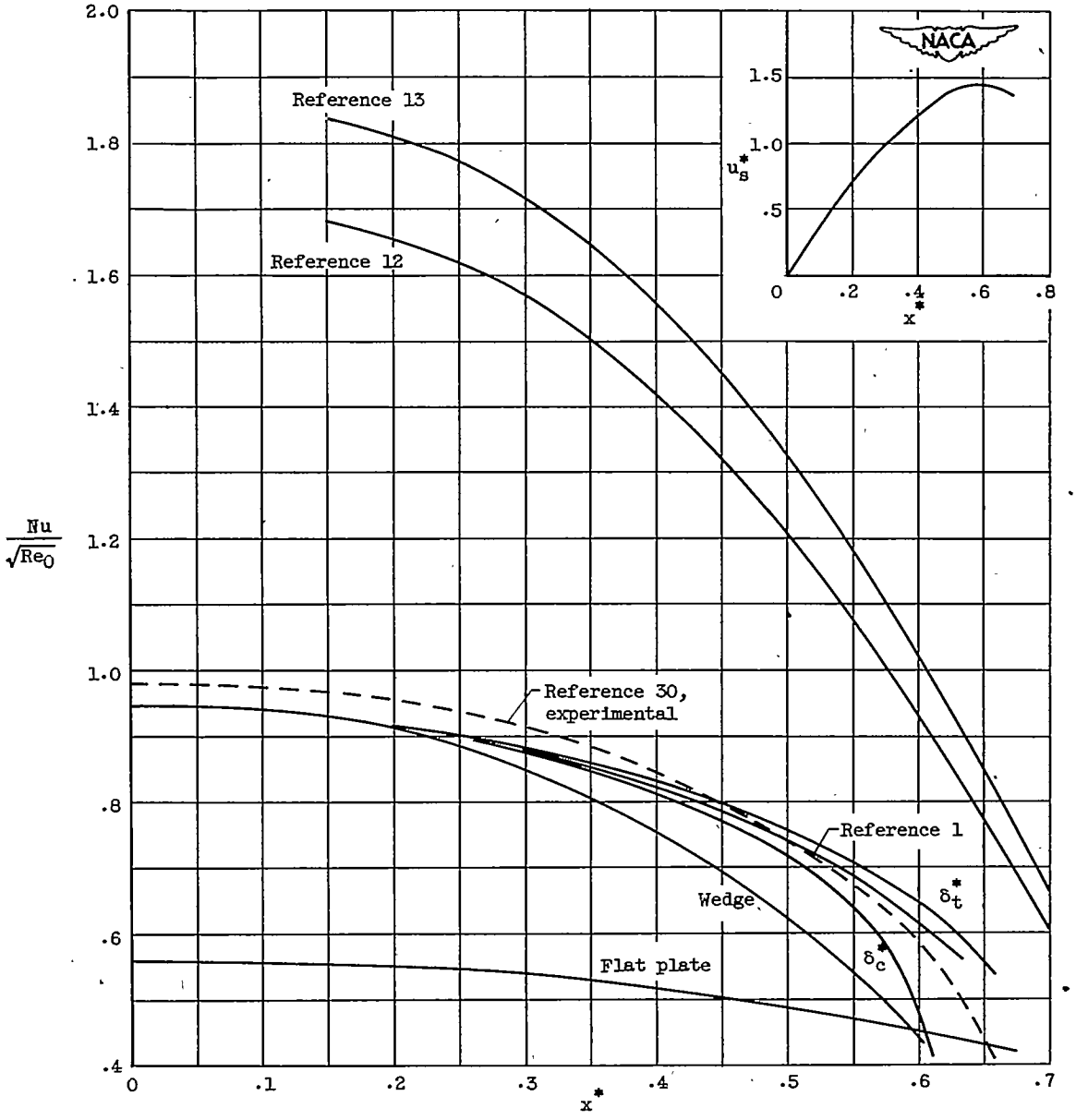

Figure 11. - Comparison of present method with formerly used methods for calculation of local heat-transfer coefficients around circular cylinder with impermeable wall. v_w^*, 0; Pr, 0.7; T_s/T_w, 1.

2447

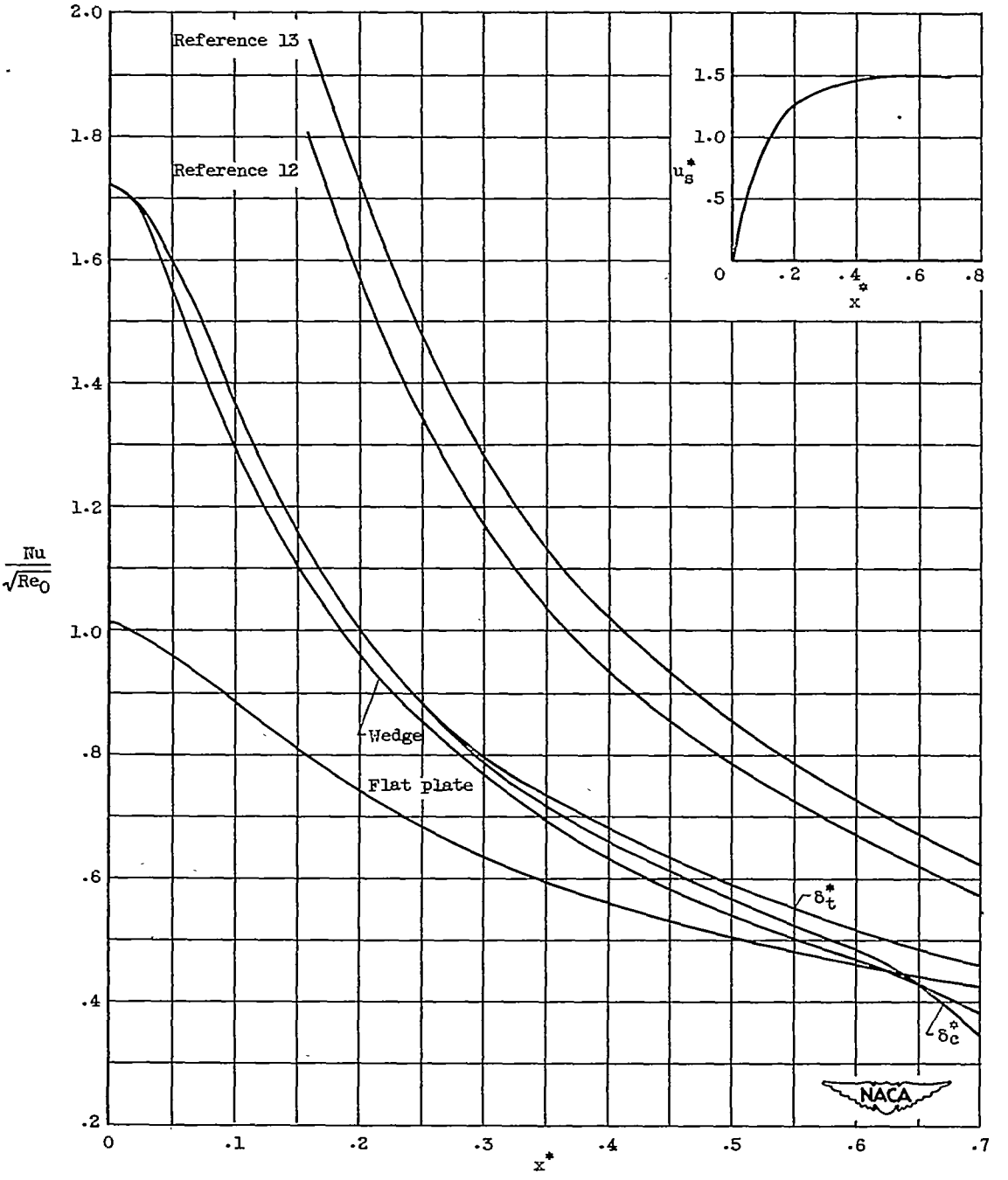

Figure 12. - Comparison of present method with formerly used methods for calculation of local heat-transfer coefficients around elliptic cylinder with axis ratio of 1:2. v_w^*, 0; Pr, 0.7; T_s/T_w, 1.

2447

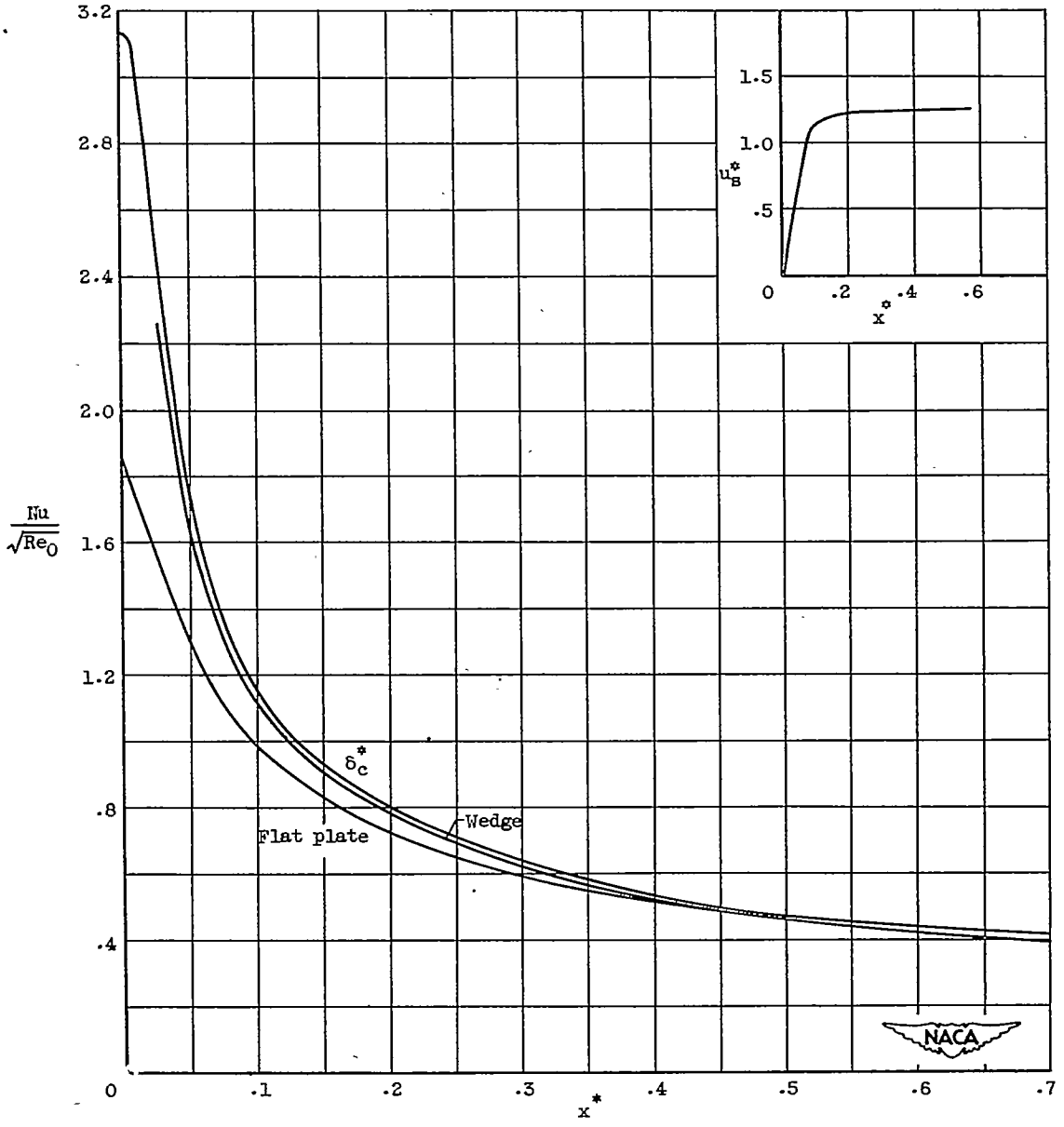

Figure 13. - Comparison of present method with formerly used methods for calculation of local heat-transfer coefficients around elliptic cylinder with axis ratio of 1:4. v_w^*, 0; Pr, 0.7; T_s/T_w, 1.

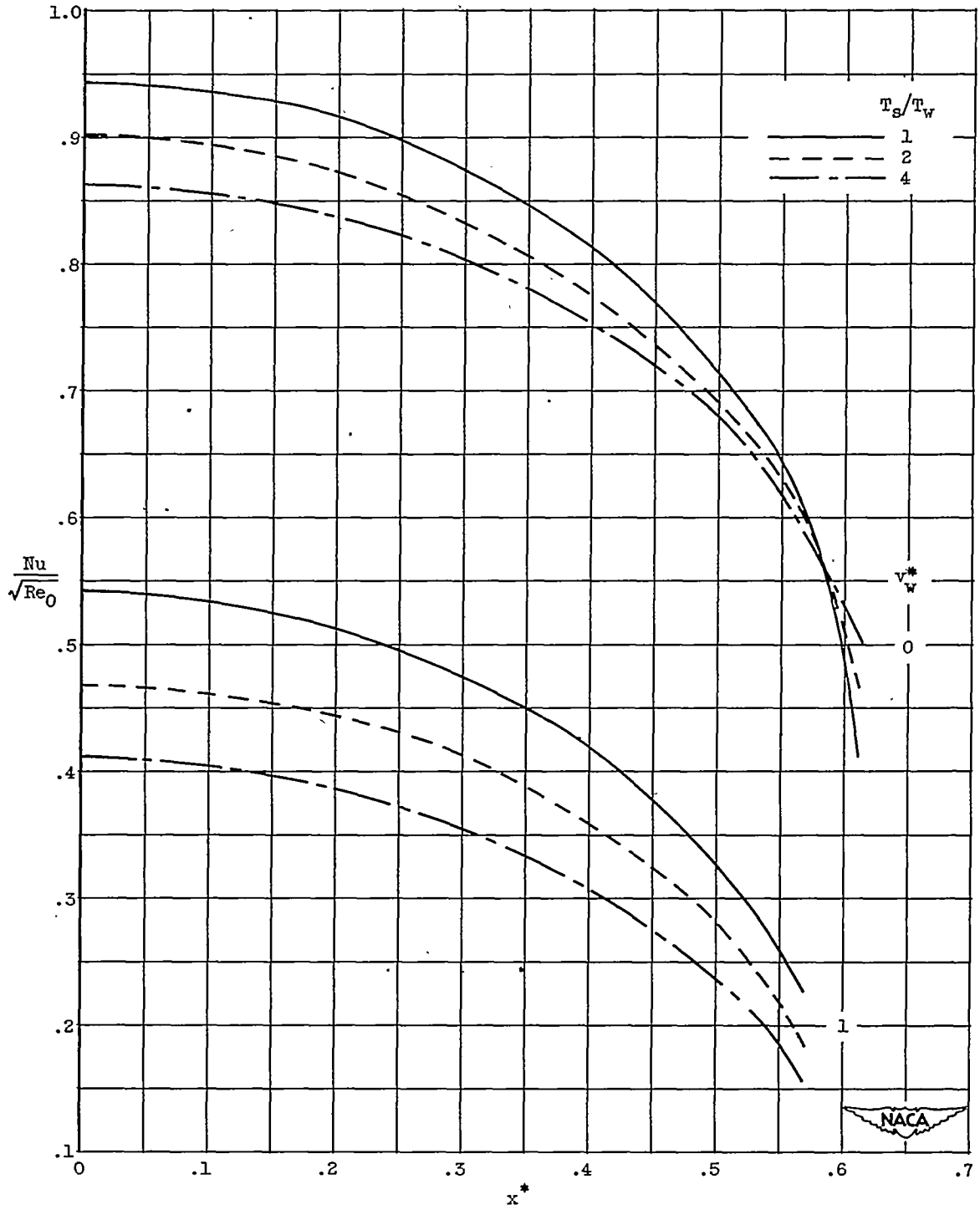

Figure 14. - Local heat-transfer coefficients around transpiration-cooled circular cylinder determined by use of dimensionless convection boundary-layer thickness for several cooling-air-flow rates and ratios of stream to wall temperature.

2447

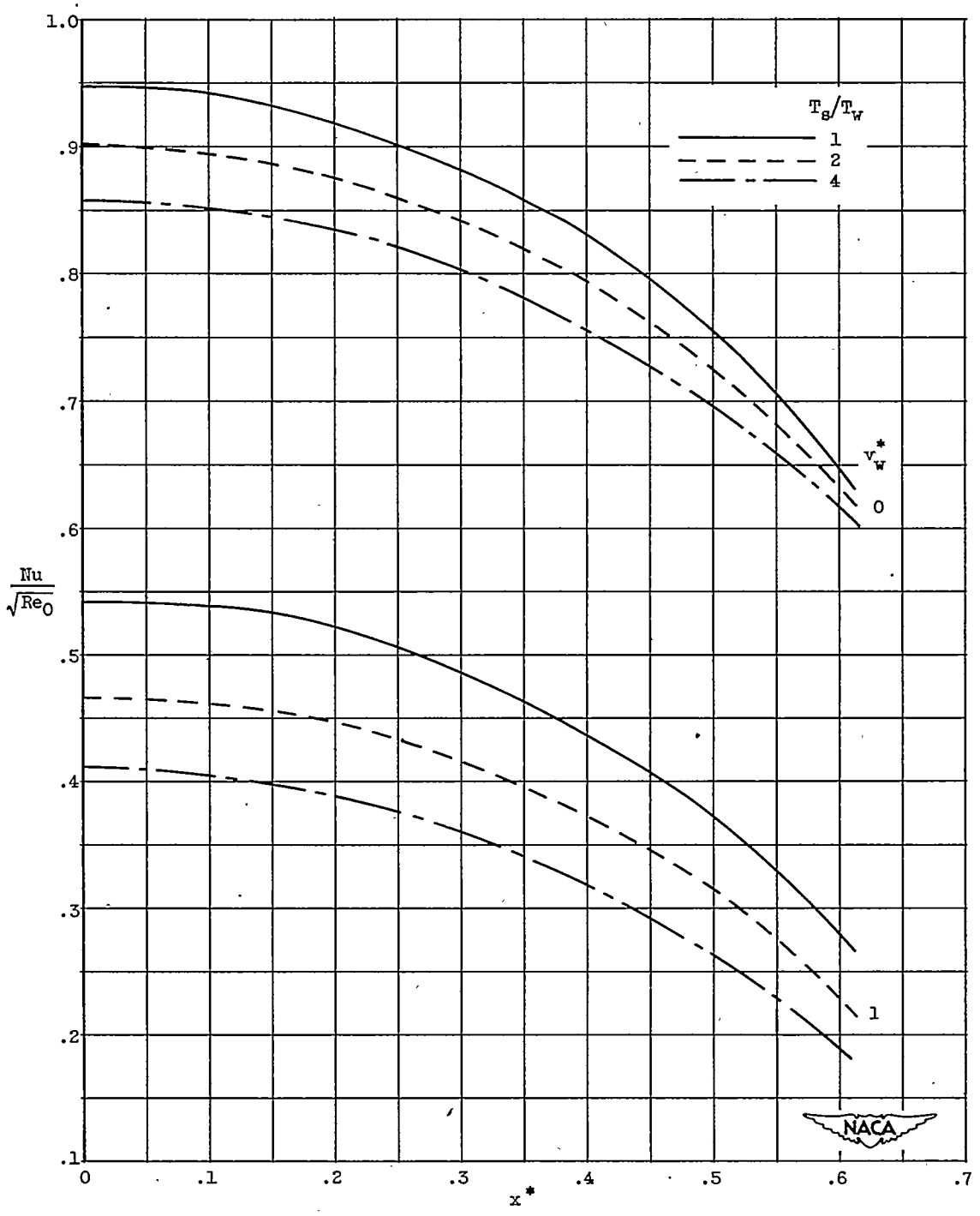

Figure 15. - Local heat-transfer coefficients around transpiration-cooled circular cylinder determined by use of dimensionless thermal boundary-layer thickness for several cooling-air-flow rates and ratios of stream to wall temperature.

2447

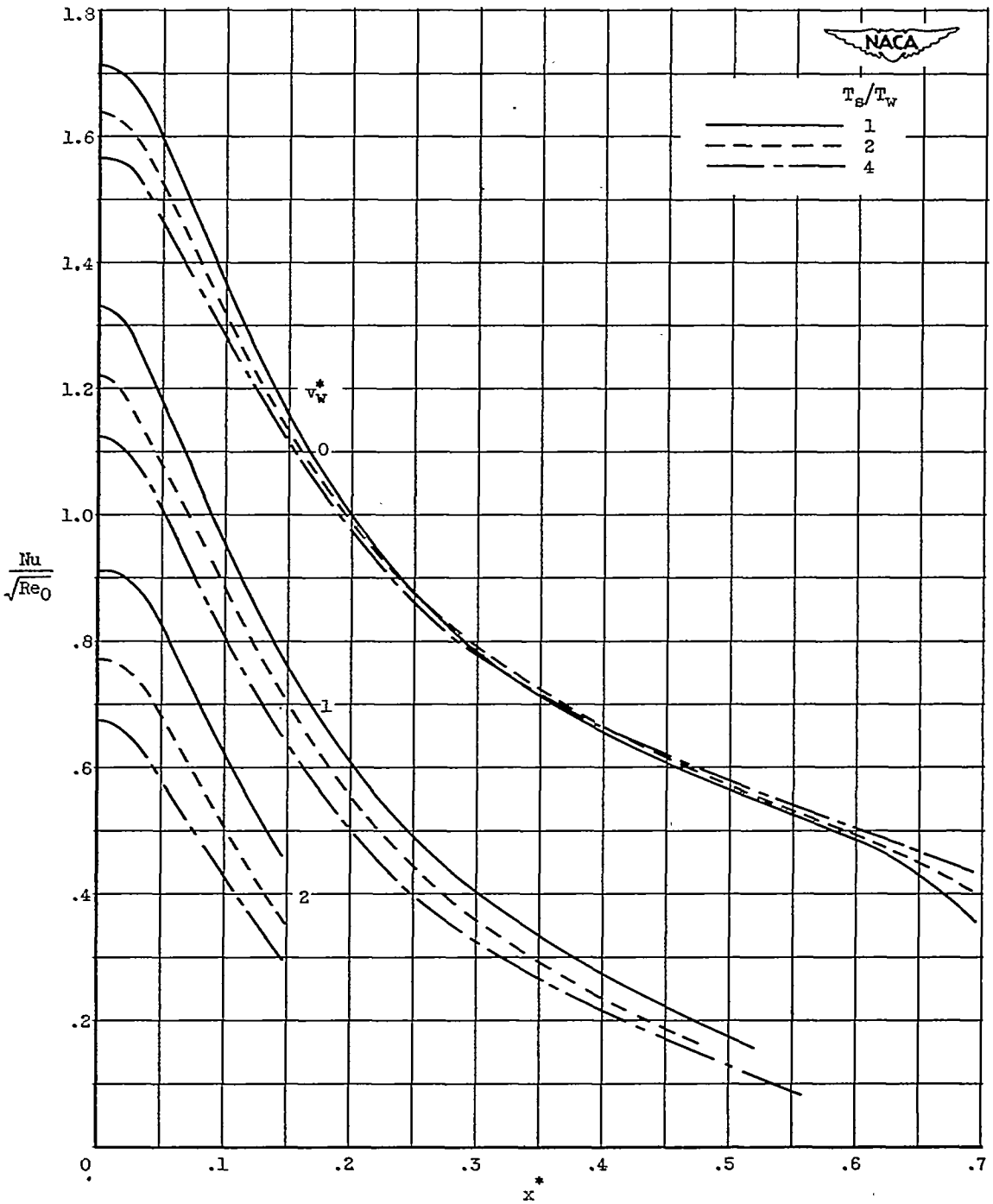

Figure 16. - Local heat-transfer coefficients around transpiration-cooled elliptic cylinder with axis ratio of 1:2 determined by use of dimensionless convection boundary-layer thickness for several cooling-air-flow rates and ratios of stream to wall temperature.

2447

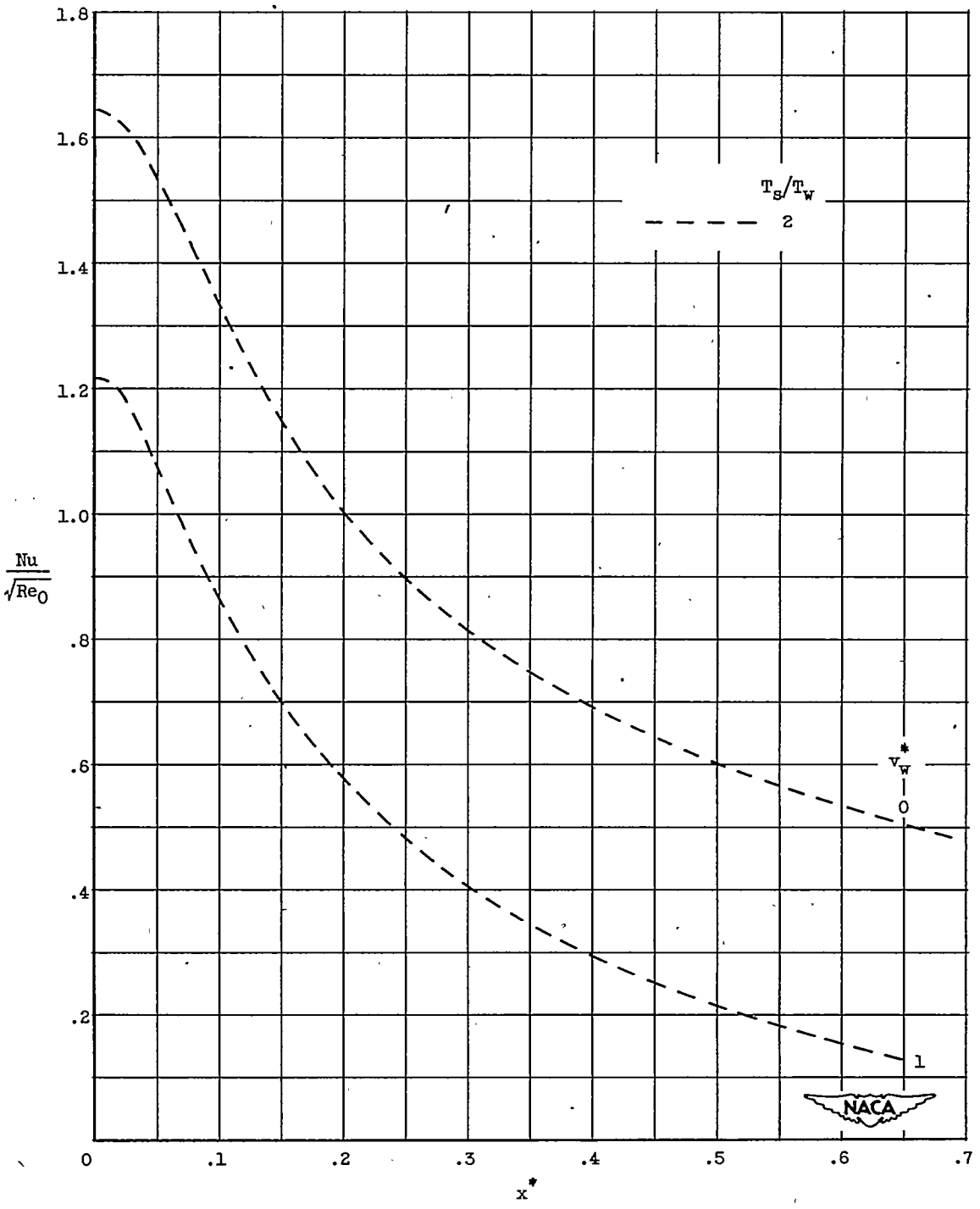

Figure 17. - Local heat-transfer coefficients around transpiration-cooled elliptic cylinder with axis ratio of 1:2 determined by use of dimensionless thermal boundary-layer thickness for several cooling-air-flow rates and ratio of stream to wall temperature of 2.

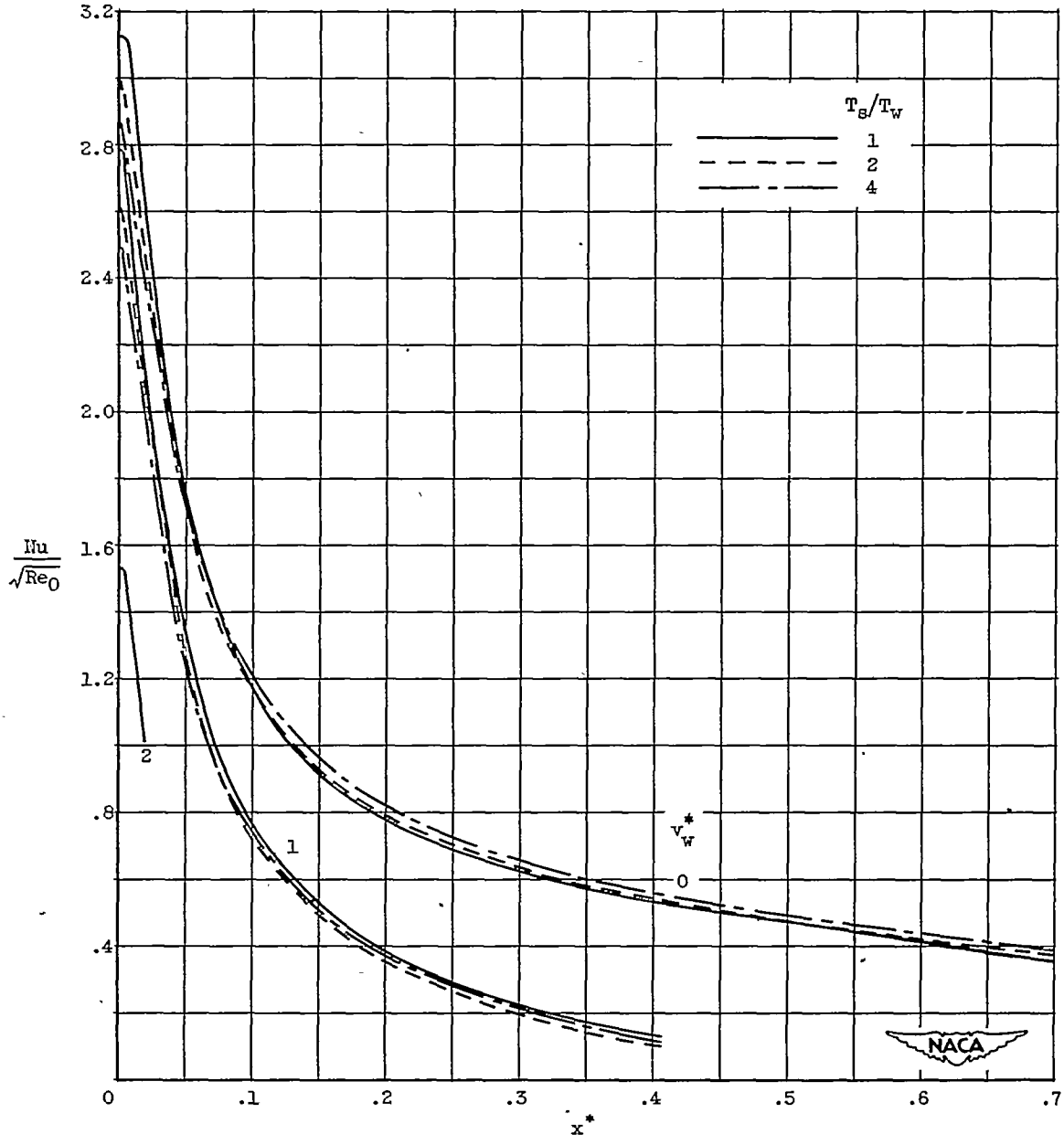

Figure 18. - Local heat-transfer coefficients around transpiration-cooled elliptic cylinder with axis ratio of 1:4 determined by use of dimensionless convection boundary-layer thickness for several cooling-air-flow rates and ratios of stream to wall temperature.

2447

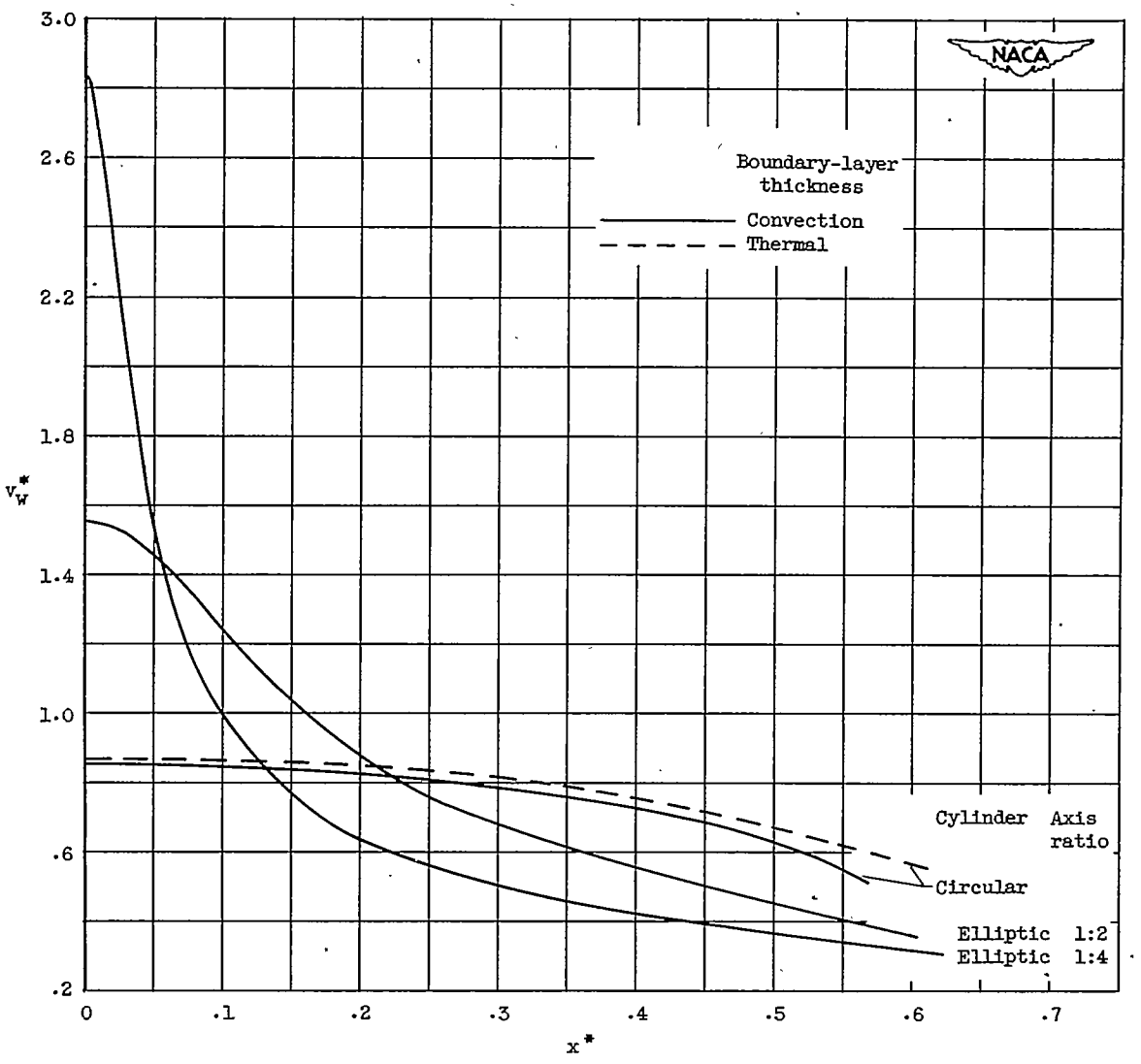

Figure 19. - Coolant flow required to maintain constant cylinder wall temperature. φ, 0.5; Pr, 0.7; T_s/T_w, 1.

2447

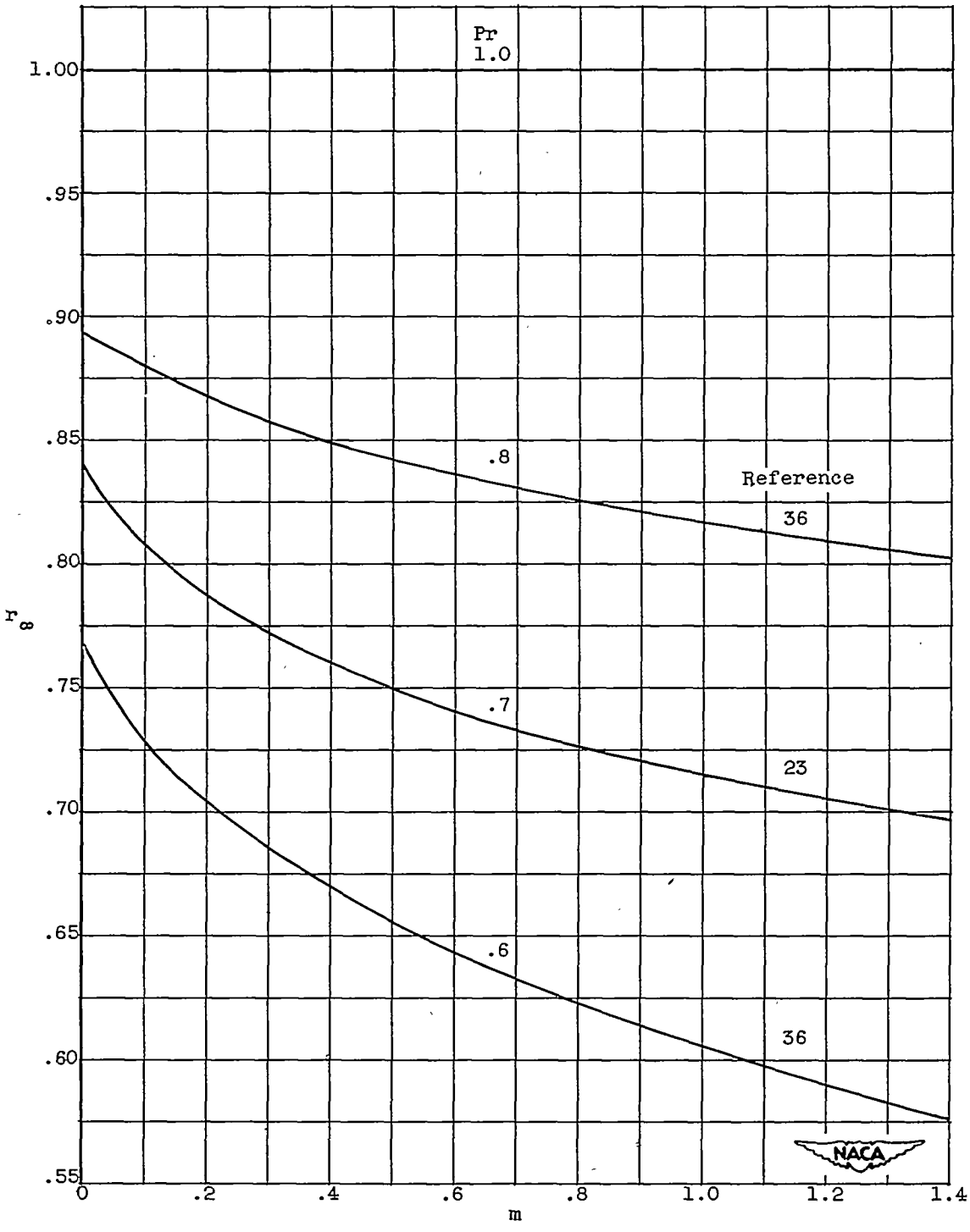

Figure 20. - Recovery factor values determining the effective temperature of a wedge.

2447

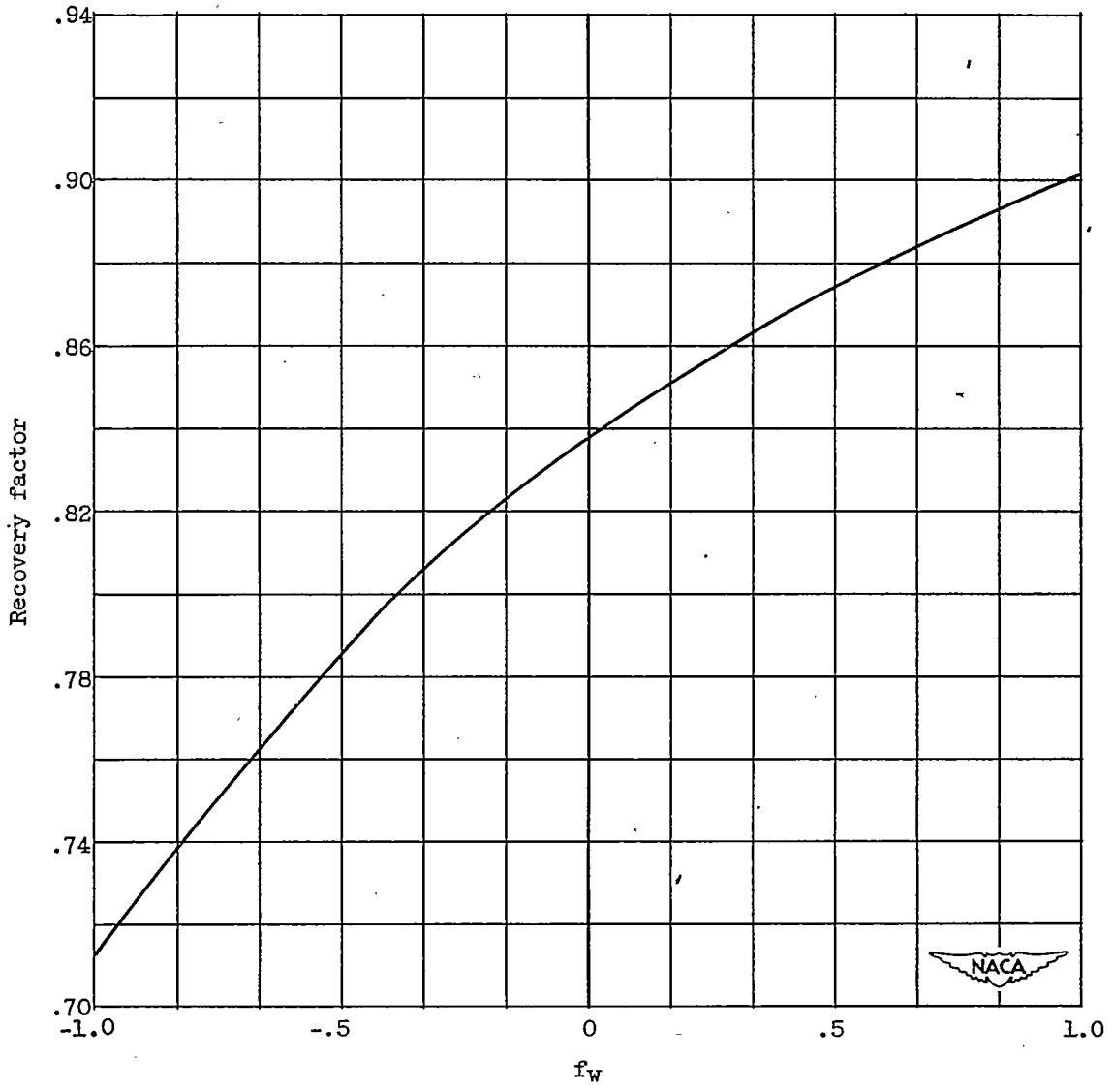

Figure 21. - Recovery factors for transpiration-cooled flat plate and constant fluid properties. T_s/T_w, 1; Pr, 0.7.

2447

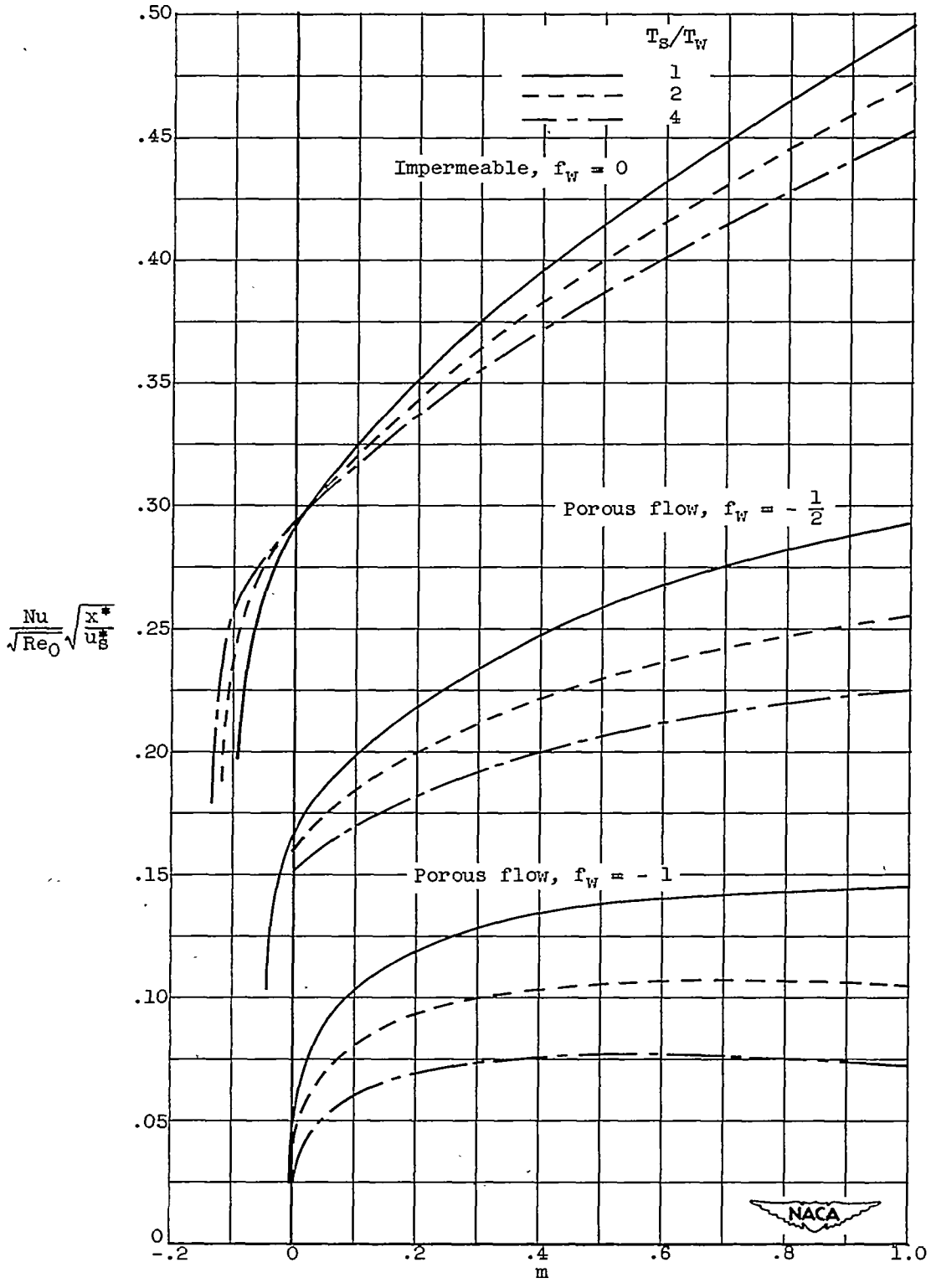

Figure 22. - Heat transfer through laminar boundary layer with and without porous flow (reference 9).

2447

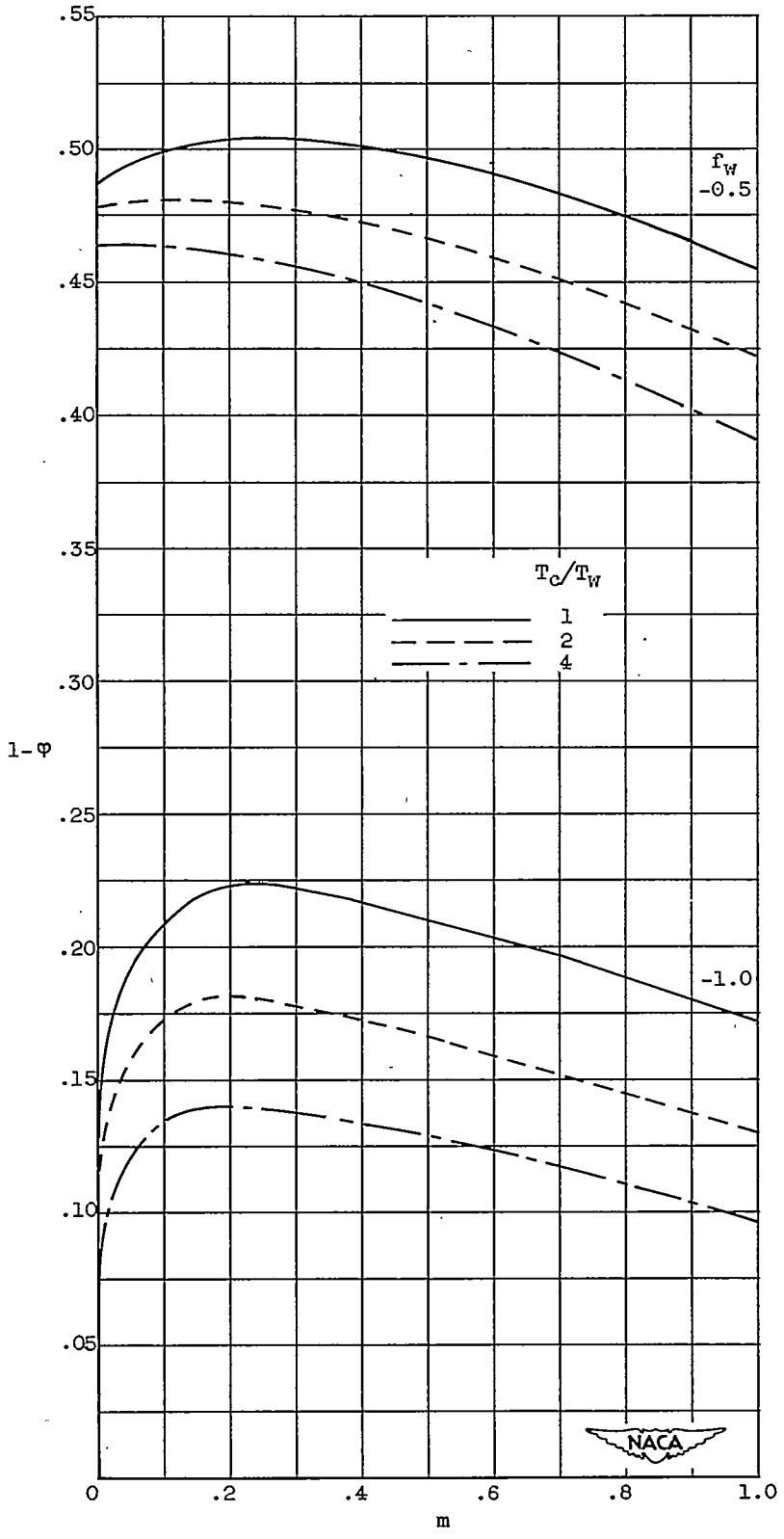

Figure 23. - Temperature of porous wall (reference 9).

NACA-Langley - 6-27-52 -1000